International Journal of Disaster Risk Reduction 128 (2025) 105747

Contents lists available at ScienceDirect

International Journal of Disaster Risk Reduction

journal homepage: www.elsevier.com/locate/ijdrr

# A multi-hazard assessment approach to reveal and compare heat- and flood-related risks and inequalities in London, Boston, and Sydney

Davide Longato [a,*], Denis Maragno [a]

[a] Department of Architecture and Arts, University IUAV of Venice, Santa Croce 191, Tolentini, 30135, Venice, Italy

ABSTRACT

Climate hazards pose several challenges to cities and their inhabitants, especially the more vulnerable ones, calling for a systematic adoption of adaptation measures. Climate risk assessments are of undoubtful importance to investigate and comprehend the nature of climate-related risks, and can ideally support adaptation planning through the identification of risk hotspots. In this study, a replicable method for assessing population risk to be negatively affected by heat stress and (river and coastal) flooding is proposed, providing a tool to support risk-based adaptive planning. Through a novel multi-hazard and multi-metric perspective and a comparative approach to reveal how they perform in terms of climate justice, the method is applied in three major cities: London, UK; Boston, US; Sydney, Australia. Results show the intra-city risk spatial variability, together with the factors that, with different magnitudes, contribute to the final risk condition. Boston has the highest proportion of population living in the most at-risk areas for heat stress. The same applies to London concerning flood risk. Sydney has the lowest shares for both. Boston and London also show greater problems of uneven distribution of risk, with the low-income residents more likely living in the riskiest areas, especially regarding heat stress. While replicability in other contexts depends on data availability, the method and its metrics are flexible to be adjusted according to different typologies of input data. The use of assessments of this type may in principle support decisions that prioritize interventions in areas where more disadvantaged people live, thus theoretically alleviating intra-city inequalities. However, proper planning and monitoring are needed to avoid reverse effects, such as gentrification processes that could lead to exacerbating existing or creating new injustices.

## 1. Introduction

Climate change, which is primarily driven by human activities such as burning fossil fuels, deforestation, and industrial processes, presents significant challenges for societies across the globe and is projected to persist and likely worsen in the future [1]. Its effects include rising temperatures, shifting precipitation patterns, rising sea levels, and ever-more extreme weather events, such as heat-waves, floods, wildfires, and droughts [2], which has already become more frequent and intense in the past decades (e.g., Ref. [3]). These events have tangible impacts on ecosystems, human activities, and people's life, possibly causing – among others – critical infrastructure disruption, physical damages to human assets, displacement of communities, and harming people's health, while disproportionately impacting marginalized, disadvantaged, and demographically vulnerable populations [4–6]. While urban areas face the same general climate risks as their surrounding regions, their unique environments can magnify or alter them [7]. Consequently, many cities worldwide are increasingly experiencing serious impacts due to extreme weather events and climate-related disasters. During and after these extreme events, the exposed population may incur health impacts, which can cause injuries, illnesses, and deaths, with most of them that could be avoided [8]. For example, very strong heatwaves in Europe occurred in 2003 and 2022, causing a peak of heat-related mortality [9,10], with many of them attributable to the overheating of urban areas due to the

* Corresponding author.
E-mail addresses: dlongato@iuav.it (D. Longato), dmaragno@iuav.it (D. Maragno).

https://doi.org/10.1016/j.ijdrr.2025.105747
Received 6 November 2024; Received in revised form 5 August 2025; Accepted 6 August 2025
Available online 6 August 2025

urban heat island (UHI) phenomenon (e.g., Ref. [9]). Notably, it has been shown that such a mortality rate can be reduced by increasing green spaces to cool down urban temperatures (e.g., a 10 % increase of tree coverage may have reduced UHI-related mortality by 10 % during past heatwaves in London [11]).

Cities thus play a crucial role in the face of climate hazards, and this role will only grow in significance given that the urban population is projected to continue increasing in the coming years. In parallel, climate change will increase urban populations' exposure to environmental risks, exacerbating existing inequality in vulnerability due to socioeconomic differences, including race, ethnicity, and income level [12]. Consequently, many cities are actively seeking ways to mitigate the consequences of these hazards, reduce vulnerabilities, and minimize negative effects by focusing on adaptation approaches – meaning taking action to prepare for and adjust to the current and projected climate impacts – that can enhance overall resilience and increase adaptive capacity.

In the context of decision-making toward climate adaptation, risk assessments are key to investigating and comprehending climate-related risks in cities, for example by identifying risk hotspot areas. In the literature, many different methods have been developed and tested for assessing climate-related risks and impacts with the (more or less explicit) aim to support risk reduction policies and decisions. These focus on different climate risks, including urban, fluvial, or coastal flood [13–16], and heat stress risk (e.g., Ref. [17–19]), and sometimes disentangle environmental and social equity issues that are key determinants in influencing people's vulnerability, exposure, and, consequently, risk (e.g., Ref. [20–23]).

Generally speaking, a risk assessment, which is purposeful to inform a particular type of decision and inherently characterized by uncertainty, can be described as a process to investigate and comprehend the nature (e.g., the multiple concurring factors), and to determine the level of risk [24]. To effectively inform the adaptation process, climate-related risk assessments should ideally be linked to the identification, planning, and prioritization of options for preventing or adapting to climate-related risks and disasters [25,26]. It is in such a discipline that a growing understanding of the interplay between hazard, vulnerability, and exposure has led to advancing risk assessment science to more comprehensive models and assessment methods [27], with risk defined as the product of hazard, vulnerability, and exposure, as also defined by IPCC [1].

In particular, when it comes to developing risk assessments, including climate risks, comprehensive vulnerability evaluations are very much needed. These must be able to investigate, interpret, and understand the different physical and socioeconomic characteristics that make up cities, and their interplay in the context of hazards [28]. This understanding is crucial for guiding the adaptation process. On the one hand, vulnerability as a biophysical condition identifies the degree of resilience of urban physical environments, which refers to the predisposition of a given territory to suffer or not (and to what extent) the impact of the hazard [29]. However, this perspective is limited, as it excludes the social, economic, political, and cultural factors that must be addressed when estimating vulnerability [30]. Some population groups (e.g., the elderly, people with chronic illnesses, people with mobility issues, the poor, and the socially isolated) are more vulnerable than others [8]. Areas identified as having high physical and social vulnerability to climate hazards (and consequent impacts) tend to have low or limited resilience, as social processes of marginalization and exclusion play an important role in unequal access to resources. The design and implementation of effective disaster risk reduction and adaptation interventions thus require attention to these inequalities in the context of ongoing social changes.

While concrete responses to societal challenges, such as climate change adaptation, are not always effectively incorporated in planning instruments for various reasons (e.g., economic, political, organizational [31]), when these are present, in many cases – especially in contexts with less human and technical resources – they are not informed by risk assessments, highlighting a rather unresolved challenge in appropriately supporting policy action through risk knowledge [32,33]. Possible causes include the strong dependence of risk evaluations on accurate and up-to-date data which, together with computational and technical complexities and uncertainties, makes it difficult to reliably apply them, as well as the "black-box" nature of many evaluations, meaning it can be difficult for policymakers to interpret and critically assess why they are predicting a particular result [34,35].

Taking these considerations into account, the overall aim of this work is to develop a replicable risk assessment method to evaluate the risk of population to be negatively affected by climate-related hazards, which can be used to support adaptation planning decisions at the city scale, showing the mechanisms underlying the construction of the assessment framework and related metrics using multi-source data and multiple assessment techniques. Specific objectives include the testing of its applicability to different climate-related hazards in multi-risk contexts, its geographical replicability in diverse data-rich environments and socio-demographic settings, and its suitability to inform comparative analyses, also in the framework of equity issues. The method is applied in three major cities located in three different continents (i.e., London, UK (Europe); Boston, US (North America); Sydney, Australia (Oceania)) to include geographically and socio-demographically different multi-cultural urban contexts in which equity issues may be a major concern. The method utilizes available socioeconomic and environmental spatially-explicit data to develop hazard, exposure, and vulnerability metrics that contribute to the final risk, in accordance with the latest IPCC's risk framework. First, the method is applied to assess population risk in case of heat stress (i.e., during a heatwave) and a major (river and coastal) flooding event in each case study city. Second, the risk assessment results are analyzed to unveil the factors that mostly contribute to the final risk condition, providing an overview of and comparing possible risk-related inequalities across the case studies.

The novelty of the work lies in.

- the multi-hazard perspective and the comparative nature used to assess the intra-city risk spatial variability and related potential inequalities across the three different cases analyzed, since most similar studies typically focus on a single city (e.g., Ref. [36]) or, even if including and comparing multiple cities, they typically focus on a single hazard (e.g., heat stress (Rocha et al., 2024; [20]));
- the use of the latest open-access socioeconomic data at the finest resolution possible concerning census-related data to depict social vulnerability (e.g., similar studies used more aggregated geographical units [37]), selected and harmonized to allow for a comparison among the cases analyzed;

- the application and combination of multiple, sometimes innovative (to our knowledge), and replicable assessment techniques and metrics, for example in the calculation of the propensity to be affected by urban heat island (UHI) effects through a purposely developed index – based on satellite data – that also considers the potential cooling effect of surrounding vegetation (see Section 2);

The remainder of the manuscript is organized as follows. Section 2 presents the case studies and the rationales for their selection, the methodological aspects of the risk assessment approach, and the steps followed to calculate and combine the hazard, exposure, and vulnerability metrics and indicators. Section 3 presents the results, including the hazard, exposure, vulnerability, and final risk maps, as well as elaborates on them to unveil and compare possible risk-related inequalities across the case studies. Section 4 discusses the results in the light of their potential to support adaptation planning processes and decisions (i.e., risk-based adaptive planning), and to unveil climate risk-related inequalities, as well as provides an overview of the challenges and limitations of the approach used. Finally, Section 5 provides the conclusions of the study.

## 2. Materials and methods

### 2.1. Case study city selection

The rationales for selecting the case study cities are.

- all cities are located in a country where the official language is English (necessary for understanding the information collected);
- they are characterized by a multi-cultural environment attracting a huge amount of people from all over the world who contribute to a highly diversified socio-demographic profile of the city, possibly causing socio-economic disparities and equity concerns that deserve special attention;
- even if with different intensities, they are all experiencing climate shifts exacerbating climate-related impacts due to climate change that pose several challenges to the city itself and its inhabitants, and call for systematic adoption of adaptation measures;
- they are highly committed to developing sustainability and resilience strategies, targeting both socio-economic and environmental sustainability aspects;
- they are characterized by a data-rich environment, allowing for in-depth investigation of environmental and socio-demographic aspects.

Three case studies located in three different continents were selected according to the abovementioned criteria to capture different socio-demographic settings, namely London (UK), Boston (US), and Sydney (Australia). In particular, the case study (administrative) boundaries correspond to the Greater London Area, the Municipality of Boston, and the Urban Agglomeration (i.e., metropolitan area) of Sydney. A brief description of the analyzed cities is provided in Supplementary Material.

All of them are actively engaged in developing plans and policies to minimize climate risks and impacts and promote climate adaptation and resilience. Above all, they are all part of the Resilient Cities Network by the Rockefeller Foundation, focused on building climate resilience city strategies.[1] In London, long-term adaptation planning and implementation aspects are integrated into existing plans and policies of the Greater London Authority, such as the London Environment Strategy, the London Plan, and the Transportation Strategy and Transportation Climate Change Adaptation Plan.[2] In recent years, the Authority has also recognized the importance of supporting these efforts with climate risk maps, commissioning climate risk assessments for both urban heat and surface water flooding that include population exposure and vulnerability factors.[3] Boston, instead, adopted purposeful adaptation plans, such as the Boston Heat Resilience Plan[4] [38] and the new 2030 Climate Action Plan,[5] which focuses on mitigation and adaptation aspects. To this aim, the Climate Ready Boston programme [39], which provides citywide climate hazard (e.g., river and coastal flooding) and vulnerability assessments (including socio-demographic determinants of vulnerability), laid the foundation to the subsequent climate actions and policies developed in the city, including additional planning efforts, policy and regulatory changes to advance adaptation across many sectors (e.g., land use and zoning regulations, open space policies, coastal resilience projects), and the formation of the Office of Climate Resilience.[6] In Sydney, the municipality developed the Cooling Sydney Strategy [40] and a climate change adaptation strategy (City of Sydney, 2017) to promote actions that combat heat and other climate risks and impacts. Such purposeful strategies integrate other existing ones, where adaptation and resilience are considered key aspects, such as the Environmental Strategy.[7]

[1] https://resilientcitiesnetwork.org/.
[2] https://www.london.gov.uk/programmes-strategies/environment-and-climate-change/climate-change/climate-adaptation/london-climate-resilience-review?ac-202105=202102.
[3] https://www.london.gov.uk/programmes-and-strategies/environment-and-climate-change/climate-change/climate-adaptation/climate-risk-map.
[4] https://www.boston.gov/departments/climate-resilience/heat-resilience-solutions-boston.
[5] https://www.boston.gov/departments/environment/boston-climate-action.
[6] https://www.boston.gov/departments/climate-resilience.
[7] https://www.cityofsydney.nsw.gov.au/strategies-action-plans/environmental-strategy.

Widening the geographical scope to the whole metropolitan and regional area in which Sydney is located, other municipalities are committed to integrating adaptation actions through several urban planning strategies and controls.[8] To support these strategies and actions, the Planning Department of the New South Wales Government recently released a heat vulnerability index, developed using canopy cover, land surface temperature, and demographic information, for the Greater Sydney area.[9]

### 2.2. Methodology

The assessment of risk is carried out for two of the most recognized climate-induced hazards that may impact the three cities, which also are among the ones projected to increase in frequency and intensity in the future and for which adaptation solutions are very much needed: i) flooding associated with river and coastal waters (as a consequence of intense rainfall and/or storm surge events) and ii) periods with high temperatures (i.e., heatwaves) that lead to heat stress/thermal discomfort conditions.

It relies on the risk factors defined by the Intergovernmental Panel on Climate Change (IPCC), which considers risk as a function of hazard, exposure, and vulnerability. According to Cardona et al. [41] and IPCC [1], hazard refers to “the potential occurrence of a natural or human-induced physical event or trend that may have adverse effects on vulnerable and exposed elements”; exposure refers to the presence of elements (including people) located “in places and settings that could be adversely affected”; vulnerability refers to “the propensity or predisposition to be adversely affected” (of the exposed elements).

Specifically, the objective of the assessment is to determine the risk of the resident population being negatively impacted when the two considered climate-induced hazards occur.

Methodological aspects of the risk assessment were defined to be replicable in all three cities, using data and metric calculation methods, and indicators that make the assessment results as comparable as possible. This especially influenced the selection of socio-demographic variables, which needed to be consistent across all three case studies. All indicators are calculated so that the higher the value, the worse the condition. Given the scope and the type of data used, the reference spatial unit for which all the metrics – and the final risk indicator – are calculated is represented by the smallest census spatial unit for which the population demographic information is provided by the official government census surveys (i.e., Lower Super Output Areas – LSOAs – in London; Block Groups – BGs – in Boston; Statistical Areas Level 1 – SA1s – in Sydney), to get the most detailed spatial resolution possible. Population demographic information is collected through the most recent decennial (or quinquennial in the case of Australia) national census surveys. Only in a few cases, data from previous censuses or other population survey sources were used, since not available in the last official census survey (more details are provided in the following sections). Table S1 in Supplementary Material shows, for each factor of the risk function, the key variables used, the rationale for using them in the risk assessments, and the data sources.

#### 2.2.1. Hazard data and metric calculations

Regarding river and coastal flooding, it was assumed a hazard event in which a major flood occurs (i.e., up to a 100-year-return-period event). Consequently, the spatial distribution of the hazard factor matches with the flood-prone areas that may be inundated during such an event. For calculating the hazard indicator, the proportion of land area (i.e., the area that usually is dry and not covered by water, thus excluding water and wetland areas – if present – according to the land use map) that is prone to flood is calculated in each census unit. The resulting percentage values are then normalized in a 0 to 1 range through the formula:

$$H_{flood,j} = \frac{flood_j - min\left(flood_j\right)}{max\left(flood_j\right) - min\left(flood_j\right)}$$

Where $flood_j$ represents the proportion of land area in the census unit $j$ that is prone to flood in a 100-year-return-period flooding event.

Concerning high temperatures, it is assumed a hazard event in which a heatwave – irrespective of the air temperature spatial variability due to local environmental conditions (e.g., mitigating effects by sea, which can cool down temperatures during daytime but increase them during nighttime, or by wind patterns) – leads to potentially dangerous heat stress/thermal discomfort conditions in the whole city area (i.e., all three cities are located in mostly flat or slightly hilly areas, thus with negligible effects in air temperature variation due to altitude). Consequently, the hazard factor is considered to be equal (i.e., the maximum) across all the city areas. The hazard indicator thus is:

$$H_{heat,j} = 1$$

Where $heat_j$ is the heat-related hazard indicator in the census unit $j$.

#### 2.2.2. Exposure data and metric calculations

For assessing the flood-related risk, population exposure is calculated considering two aspects. The first concerns the number of people living in an area. The second is related to the hypothetical temporal duration of the human presence according to the different land uses located in flood-prone areas, an additional exposure factor that considers the degree of occupancy of the land that might

[8] https://www.planning.nsw.gov.au/policy-and-legislation/resilience-and-natural-hazard-risk/urban-heat/cooler-places/using-planning-strategies-and-controls-for-cooling.

[9] https://www.planning.nsw.gov.au/policy-and-legislation/urban-greening/urban-heat-and-canopy-data.

influence people's temporal exposure (i.e., people tend to stay more time in specific land uses such as in their residences or workplaces than in others involving more temporary activities such as urban parks and roads). Various methods exist for estimating this aspect (e. g., occupancy degree at various times of day and/or working days vs. non-working days), mostly involving a qualitative (expert-based) estimation through scoring systems (e.g., Ref. [42]). In this assessment, a simplified method (i.e., without considering different times of day or week) based on a quick estimation of the overall degree of temporal occupancy in different land uses through a 0 to 1 scoring system (i.e., 0 – no or negligible presence; 1 – maximum temporal presence potential) is proposed based on a method and scores elaborated by experts within an Italian flood risk management plan (i.e., [43])). After careful checking and validation by the authors, these scores have been considered sufficiently reliable to be used in the three cities analyzed, since they are developed by experts in the field and – after proper data harmonization – suitable to land use categories that can be typically found in many contexts (including those analyzed in this study). The scores assigned to the different land uses in the three cities are reported in Table S2 in Supplementary Material, together with their spatial distribution (Fig. S1). The average score for each census unit is then calculated according to the proportion of the different land uses that fall within a flood-prone area (if present).

To calculate the flood-related exposure indicator, data are finally normalized (in a 0 to 1 range) and combined through the formula:

$$E_{pop.time,j} = \frac{pop_j - min\left(pop_j\right)}{max\left(pop_j\right) - min\left(pop_j\right)} * \frac{time_j - min(time_j)}{max(time_j) - min(time_j)}$$

Where $pop_j$ represents the number of people living in the census unit $j$, and $time_j$ represents the indicator that qualitatively describes the hypothetical average temporal presence of people over the flood-prone area of the census unit $j$.

Concerning the heat-related risk assessment, population exposure is instead calculated based on the number of residents only, through the normalization formula:

$$E_{pop,j} = \frac{pop_j - min\left(pop_j\right)}{max\left(pop_j\right) - min\left(pop_j\right)}$$

Where $pop_j$ represents the number of people living in the census unit $j$.

### 2.2.3. Vulnerability data and metric calculations

Population vulnerability is assessed based on the sociodemographic characteristics that may make certain population groups more likely to be negatively impacted (e.g., in terms of health and/or economic impacts) because of their lesser ability to prepare for, respond to, and recover from climate-induced impacts. Considering their availability in all three case studies, the socio-demographic variables selected to represent the more vulnerable population groups are: proportion of young children <5 and the elderly >65 years old; proportion of people belonging to ethnic minorities; proportion of households with low to null proficiency in speaking English; proportion of renter households; and household median income. These variables are among the most frequently used and widely accepted for their robustness in depicting population vulnerability (including to climate impacts) linked to socio-demographic factors [44,45]. Even if not including many variables such as in other studies (e.g., Ref. [46]), it has been shown that fewer, informative variables can be similarly effective in predicting social vulnerability when carefully selected (e.g., Ref. [47,48]). Despite vulnerability is claimed to be context-dependent, as it generally manifests differently across different areas [49], the variables selected in this study identify population groups that can be objectively considered more vulnerable independently of the geographical and socioeconomic context. As a further confirmation of the reliability of this selection, these variables are among the ones used to support climate risk reduction policies in two of the analyzed cities, namely London ([50]: 3) and Boston (City of Boston, 2016: 30–31). Table S1 in Supplementary Material provides the full descriptions of the rationales for using the selected variables. Once collected all the variables' data, the vulnerability indicator is calculated by normalizing (in a 0 to 1 range) and aggregating the single socio-demographic variables through the formula:

$$V_{soc,j} = \frac{\frac{V_{age,j} - min\left(V_{age,j}\right)}{max\left(V_{age,j}\right) - min\left(V_{age,j}\right)} + \frac{V_{ethn,j} - min\left(V_{ethn,j}\right)}{max\left(V_{ethn,j}\right) - min\left(V_{ethn,j}\right)} + \frac{V_{lang,j} - min\left(V_{lang,j}\right)}{max\left(V_{lang,j}\right) - min\left(V_{lang,j}\right)} + \frac{V_{ten,j} - min\left(V_{ten,j}\right)}{max\left(V_{ten,j}\right) - min\left(V_{ten,j}\right)} + \left[1 - \frac{V_{inc,j} - min\left(V_{inc,j}\right)}{max\left(V_{inc,j}\right) - min\left(V_{inc,j}\right)}\right]}{5}$$

Where $age_j$, $ethn_j$, $lang_j$, and $ten_j$ represent the proportion of vulnerable people or households living in the census unit $j$ that are considered more vulnerable according to their age, ethnicity, language spoken, and tenure situation, respectively, while $inc_j$ represents the value of the median household income in the census unit $j$.

While the vulnerability indicator solely based on the socio-demographic profile of the population is used for assessing the flood-related risk, in the heat-related assessment an additional vulnerability factor is added to account for the spatial variability of the potential overheating effects due to UHI. This factor is added because people living in areas more prone to UHI may be more vulnerable during periods with high temperatures given that they are likely to experience more prolonged heat stress/thermal discomfort conditions since this phenomenon occurs especially during nighttime, maintaining high temperatures even when they should naturally decrease to more tolerable levels (e.g., the longer the temporal exposure to heat stress conditions, the lesser is the people's ability to cool off and the recovery time for the body and, consequently, the higher is the probability of health impacts; as well as, the longer the time with high ambient temperatures, the longer the time artificial air conditioning systems are required to function leading to more energy consumption and energy bill increase [51,52]).

To this aim, a specific pixel-based indicator that qualitatively assesses the spatial variability of the vulnerability to UHI, intended as the propensity to be interested by more or less intense UHI effects, is developed using a replicable approach that combines freely accessible satellite-derived data. According to Longato and Maragno [53], this propensity is assessed based on the potential local overheating driven by the heat released by surfaces (measured through the proxy data of Land Surface Temperature (LST)) and the cooling effects possibly offered by surrounding vegetated areas (measured through the proxy data of Normalized Difference Vegetation Index). The Landsat 8 satellite is used since it provides the finest thermal data (detected at 100m resolution, downscaled at 30m resolution) among the non-commercial satellites. The detailed methodology and formula used for calculating this indicator are provided in Supplementary Material.

It has to be noted that some studies use the LST as a hazard component (i.e., proxy of urban temperature variation to simulate UHI effects) in heat stress risk assessments (e.g., Ref. [22]). However, we include it in the vulnerability component, together with the NDVI (as done by other authors (e.g., Ref. [54])), since we don't use it as a proxy to capture actual urban air temperature variations to derive heat islands as a climate hazard factor. Instead, the proposed index seeks to capture a predictive physical sensitivity/vulnerability aspect of the urban environment that can influence UHI spatial variation and intensity based on local LST interaction with surrounding vegetation (and related cooling effects).

Many studies indeed warn about the limitations of LST to properly reflect the spatially varying intensity of UHI, claiming that it is not able to fully capture the thermal dynamics driven by the complex thermal interactions between urban and vegetated land covers – generated across a wider area surrounding a specific location – and the consequent air mixing mechanisms occurring in the air layers above the surface ([55]; various authors in Ref. [56]). Using LST as the sole proxy of urban air temperature variation in urban heat risk assessments could therefore be misleading in informing effective mitigation strategies [57,58], given their non-linear relationship that leads to frequent overestimations of UHI effects by LST (e.g., Ref. [58,59]). The average value of the proposed pixel-based UHI--vulnerability-related indicator is then calculated in each census unit to estimate the census area's propensity to be interested by UHI effects. The formula for calculating the final vulnerability indicator to use in the heat-related risk assessment is calculated by combining the vulnerability indicator related to the socio-demographic profile (the one also used in the flood-related assessment) with the one (normalized in a 0 to 1 range) related to the UHI vulnerability profile of the census units, namely:

$$V_{soc.UHI,j} = \frac{V_{soc,j} + \frac{V_{UHI,j} - min\left(V_{UHI,j}\right)}{max\left(V_{UHI,j}\right) - min\left(V_{UHI,j}\right)}}{2}$$

Where $soc_j$ represents the social vulnerability indicator that combines the five socio-demographic variables selected to assess the

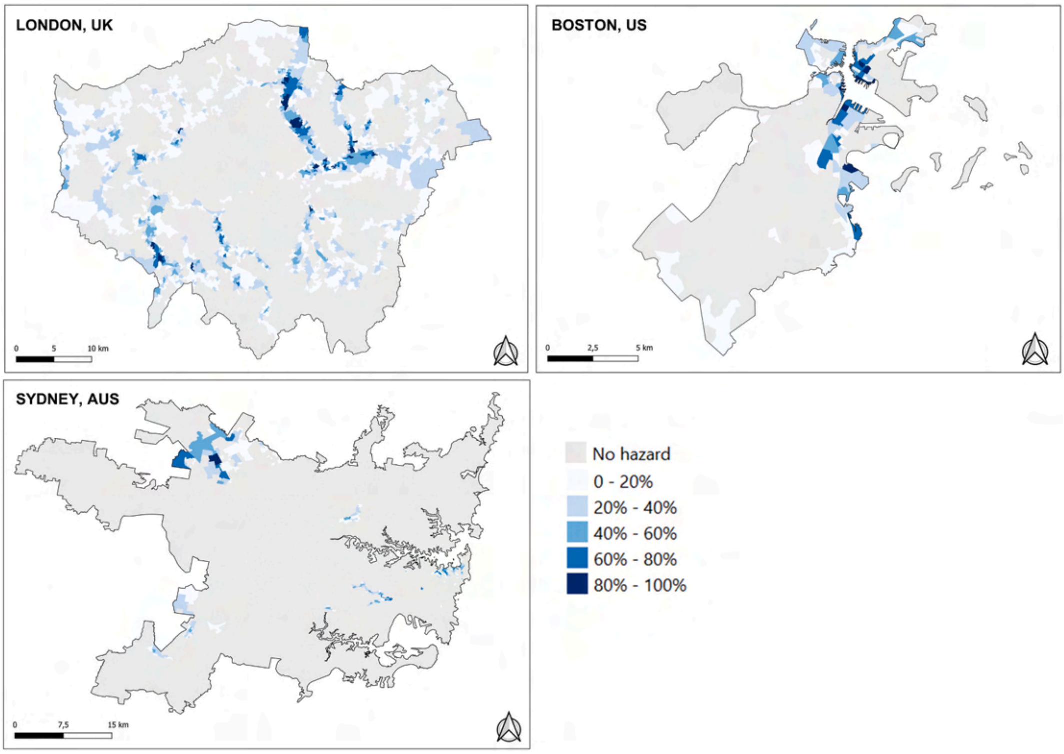


**Fig. 1.** Spatial distribution of the five percentile classes related to the flood hazard indicator (i.e., the higher the percentile class, the higher the hazard).

presence of the more vulnerable population groups in the census unit *j*, $UHI_j$ represents the average value of the pixel-based UHI-vulnerability-related indicators in the census unit *j*.

#### 2.2.4. Final risk assessment

Once calculated all the indicators related to the three factors that concur to determining the risk condition (i.e., hazard, exposure, and vulnerability), the final risk is assessed by combining them.

As concern the final flood-related risk indicator, the formula is:

$$R_{flood,j} = H_{flood,j} * E_{pop.time,j} * V_{soc,j}$$

Where $H_{flood,j}$ represents the flood hazard indicator, $E_{pop.flood,j}$ represents the population exposure indicator based on the number of resident people and the temporal dimension of human presence in the flood-prone area in the census unit *j*, and $V_{soc,j}$ represents the vulnerability indicator based on the population socio-demographic profile in census unit *j*.

Regarding the final heat-related risk indicator, the formula is:

$$R_{heat,j} = H_{heat,j} * E_{pop,j} * V_{soc.UHI,j}$$

Where $H_{heat,j}$ represents the hazard indicator related to high temperatures, $E_{pop,j}$ represents the population exposure indicator based on the number of resident people in the census unit *j*, and $V_{soc-UHI,j}$ represents the vulnerability indicator based on the population socio-demographic profile and the propensity to suffer from UHI effects in census unit *j*.

## 3. Results

### 3.1. Hazard spatial distribution

While the hazard indicator related to the heat stress risk was considered to be equal (i.e., the maximum) across all the city areas, the one concerning river and coastal flooding shows spatial variations according to the share of (usually dry) area that may be inundated during a 100-year-return-period event in each census unit (Fig. 1). In London, the more hazardous areas are found north-east and south-west of the city center along some minor rivers that are tributaries of the main river Thames, which flows through the central part of the city. In Boston, these are especially located towards the coastal area, with some coastal sections particularly exposed to coastal flooding during strong storms. In Sydney, the most problematic areas are instead found towards the northeastern inland part of

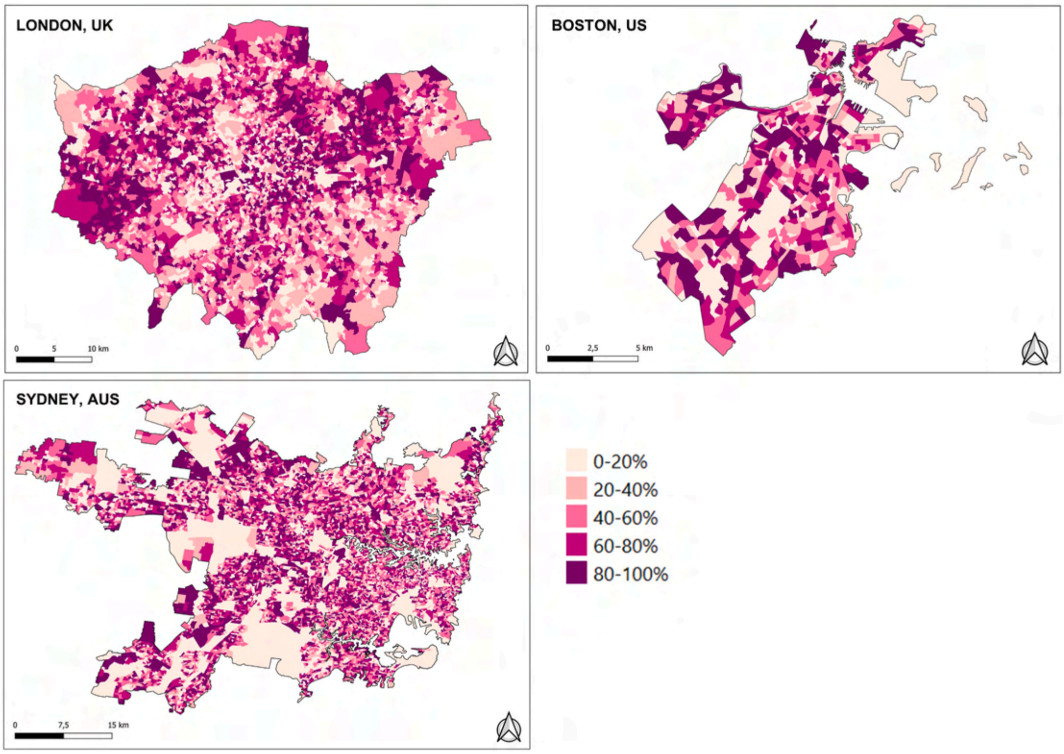


**Fig. 2.** Spatial distribution of the five percentile classes related to the heat-stress-related population exposure indicator (i.e., the higher the percentile class, the higher the exposure).

the metropolitan area, where some major creeks are located. The spatial distribution of flood-prone areas in such a flooding event, according to the official national government data, is provided in Supplementary Material (Fig. S2).

### 3.2. Exposure spatial distribution

As regards the heat stress assessment, the exposure indicator reflects the distribution of population according to the number of residents, with higher values (i.e., higher exposure due to the greater number of potentially exposed residents) that are quite widespread in all three cities, but with a tendency to be especially concentrated in areas that are external the city core where the residential use is more predominant (Fig. 2).

The composite exposure indicator related to flooding instead takes into account - besides the resident population count - also the hypothetical duration of human presence according to the different land uses that fall within the portion of the census unit that is exposed to flooding (see Fig. S3 in Supplementary Material for the mapping of this intermediate indicator). The most exposed areas are consequently the ones having a higher number of residents and, at the same time, a higher proportion of flood-prone areas that affect the land uses characterized by a higher hypothetical temporal duration of human presence (e.g., residential, public buildings/services) (Fig. 3).

### 3.3. Vulnerability spatial distribution

The vulnerability indicator relative to heat stress is a composite indicator that considers both the socio-demographic characteristics (i.e., aggregating five specific characteristics, see Figs. S4–S8 in Supplementary Material for their mapping) of the resident population that can make them more vulnerable to climate-related impacts (i.e., social vulnerability indicator) (Fig. 4) and the census unit's average propensity to be interested by overheating effects due to the UHI phenomenon (i.e., UHI vulnerability indicator) (Fig. 5; see Figs. S9–S11 in Supplementary Material for the mapping of the intermediate indicators used for the calculation of the UHI vulnerability indicator).

Concerning the social vulnerability indicator (which also represents the vulnerability indicator used in the flood risk assessment) in all three cities we can recognize well-clustered areas of high vulnerability conditions, with London and Boston having social vulnerability hotspots especially concentrated in the outskirts, while Sydney having them concentrated in more central zones of the metropolitan area. As regards the UHI vulnerability indicator, all three cities show vulnerability hotspots towards the central areas, especially Boston, which is characterized by a clear north-to-south (i.e., city center to city outskirts) gradient of vulnerability. In London, these hotspots are also spread in some outskirt areas, while some central zones are characterized by lower vulnerability

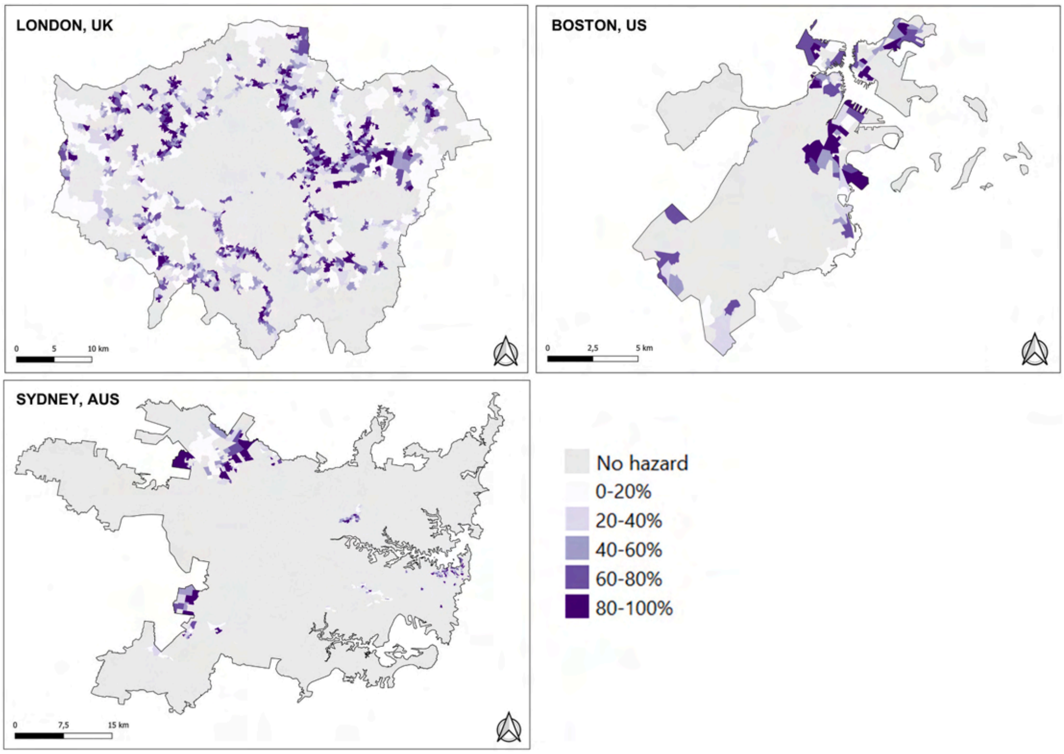


**Fig. 3.** Spatial distribution of the five percentile classes related to the flood-related population exposure indicator (i.e., the higher the percentile class, the higher the exposure).

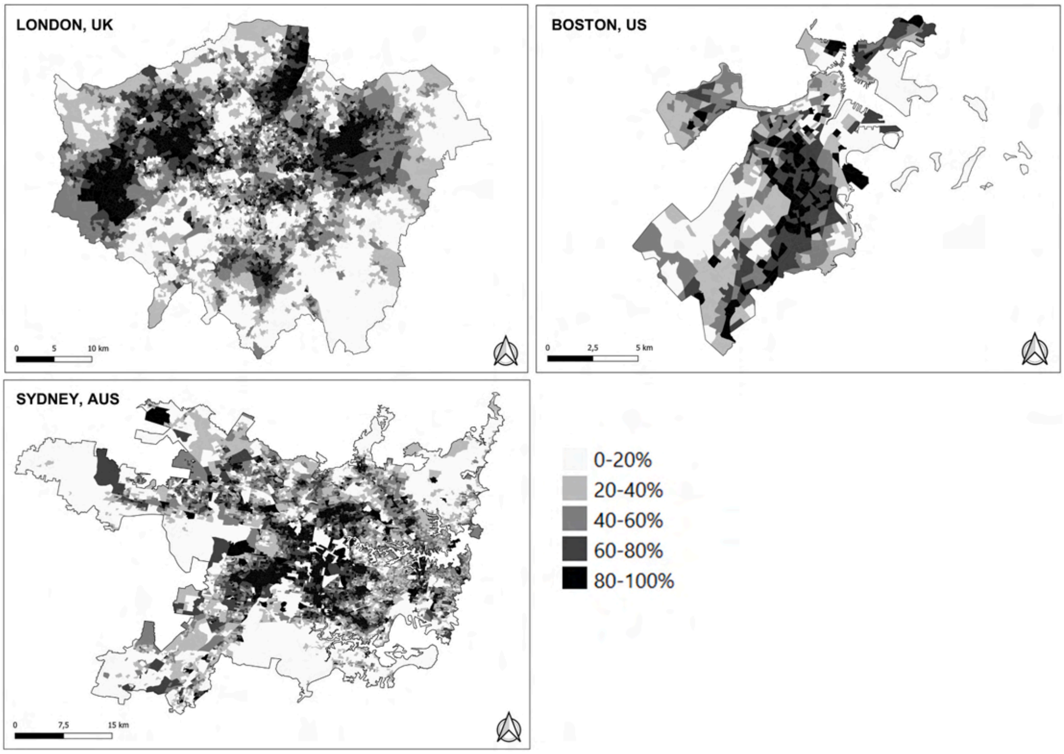


**Fig. 4.** Spatial distribution of the five percentile classes related to the social vulnerability indicator (i.e., the higher the percentile class, the higher the vulnerability).

conditions because of the presence of large parks. In Sydney, many areas in the western part of the metropolitan region also show UHI issues.

According to the spatial variability of the final heat stress vulnerability indicator (Fig. 6), all three cities are characterized by pretty clearly clustered areas characterized by higher vulnerability conditions. In London, these are especially concentrated in the eastern and western outskirts. In Boston, vulnerability hotspots are found south of the central business district and towards the more peripheral areas in the eastern and northern parts of the municipality. In Sydney, they are concentrated mainly close to the city core and the coastal surroundings, and towards the western part of the metropolitan area. More isolated vulnerability hotspot areas are however found in other widespread locations in all three cities.

### 3.4. *Final risk spatial distribution*

The spatial distribution of the two final risk indicators is shown in Fig. 7 (heat stress risk) and Fig. 8 (flood risk)

The riskier conditions for the population concerning heat stress in London are mostly found in the eastern/north-eastern sector of the city and towards the western outskirts, close to the Heathrow airport, as somewhat confirmed by the risk map developed by Bloomberg Associates [50] using several different metrics and aggregation methods. In Boston are quite scattered, with a slight predominance south and east of the central business district area. In Sydney are especially concentrated in the western/north-western inland part of the inhabited metropolitan area and, to a lesser extent, in some central and coastal zones, rather in line with the assessment by Wang and colleagues [22], who however used a partly different assessment approach and population data.

Concerning flood risk, the riskier conditions for population in London are along a couple of minor rivers flowing in the north-eastern sector of the city. In Boston are located southwest the central area and close to the Boston International Airport (north-eastern city area). In Sydney, where the flood-prone areas are more rarefied, a few hotspots of higher risk conditions are found along a coastal portion west of the city center and in some spots in the most eastern part of the metropolitan area along some major creeks.

Considering only the census units that are characterized by the highest risk condition (i.e., highest risk class corresponding to risk indicator values above the 80th percentile) for both the hazards analyzed, London has the highest percentage of overlapping census units (92 out of 4994, corresponding to 1,8 %), followed by Boston (9 out of 581, corresponding to 1,5 %) and Sydney (19 out of 10827, corresponding to 0,2 %).

### 3.5. *Risk conditions of the exposed population*

In this section, a more in-depth analysis of the final risk distribution and of the underlying factors that contribute to its variability is

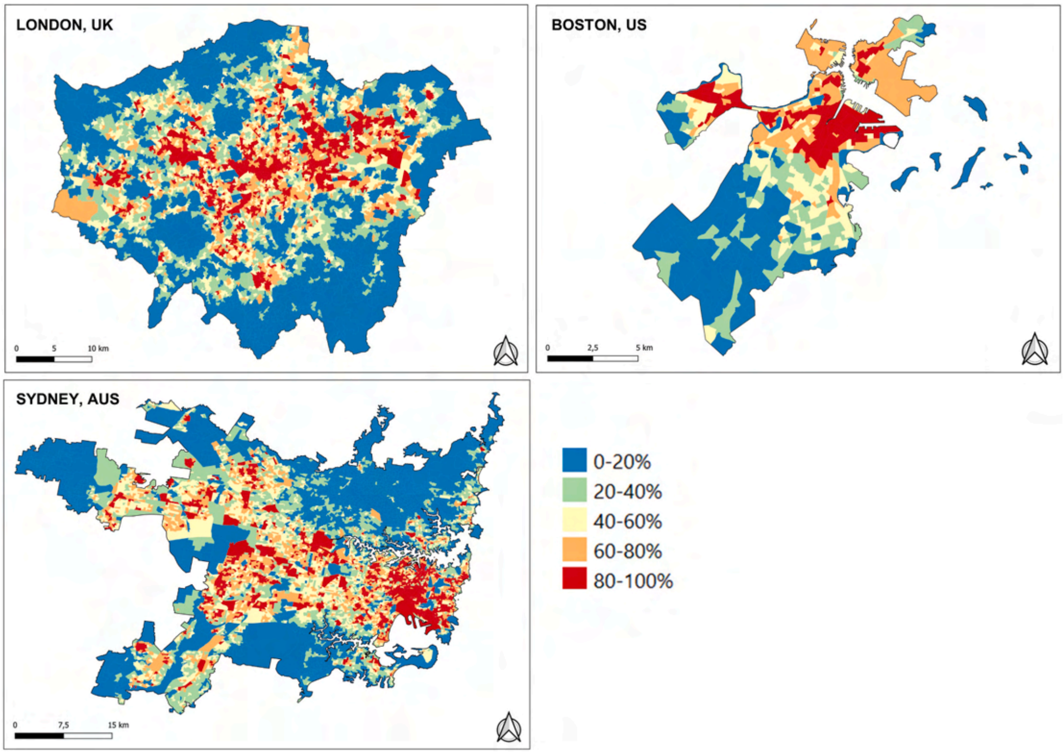


**Fig. 5.** Spatial distribution of the five percentile classes related to the UHI vulnerability indicator (i.e., the higher the percentile class, the higher the vulnerability).

presented to reveal both the risk conditions of the city's inhabitants and the existence of possible correlations with the environmental and socio-demographic variables of the exposed areas in which they live that may lead to climate- and environmental-inequalities.

Fig. 9 shows the proportion of resident population living in the different risk conditions according to the five percentile classes of the risk indicator, with the lowest percentile (0–20) indicating the lowest risk condition and the highest percentile (80–100) the highest risk condition. Concerning the heat stress risk, Boston is characterized by the highest proportion of inhabitants (>30 %) who live in the riskiest areas of the city. While London and Sydney show similar proportions (around 22 %), the latter performs better in terms of the share of inhabitants living in the least risky areas. However, if considering the areas characterized by the two highest percentile classes, a greater proportion of the population lives in such areas in Sydney. As regards flood risk, due to the greater hazard extent, London shows the highest proportion of people that live in (more or less) risky areas (i.e., nearly 78 % of population lives in no-risk areas), followed by Boston and Sydney (i.e., nearly 83 % and 97 % of population living in no risk areas, respectively). London and Boston also show a similar proportion (around 4 %) of people living in the riskier zones, while Sydney shows very much less (0,5 %).

According to Fig. 10, when it comes to areas that are characterized by the highest risk condition for both the hazards (i.e., highest multi-risk), even if not having the highest percentage of overlapping census units among the three cities (see previous section), Boston is the city in which a higher proportion of its inhabitants live in such multi-risk areas (2,5 %), followed by London (2,3 %) and Sydney (0,3 %). Concerning the proportion of inhabitants living in areas without any highest risk condition, it is the contrary, with Sydney showing the highest value (78 %), followed by London (76 %) and Boston (68 %).

To analyze how and how much the different socio-demographic and environmental variables (belonging to hazard - when present, exposure, and vulnerability factors) included in the risk assessments are correlated with the final risk condition in each city, a correlation analysis was performed. The resulting correlation matrix is provided in Figs. 11 and 13 for heat stress and flood risk, respectively. In London, the exposure factor (i.e., resident population) is less prominent than the vulnerability factor (i.e., overall population vulnerability) in determining the final risk condition concerning heat stress, while in Boston and Sydney it is the contrary. When it comes to flood risk, the situation is reversed, with a greater (positive) correlation of the vulnerability factor with respect to the (overall) population exposure in London, while in Boston and Sydney it is the exposure factor that shows a slightly higher correlation. In general, both exposure and vulnerability correlation values in the flood risk assessment are significantly lower than those in the heat stress risk assessment, meaning that they are less correlated with the final flood risk condition, which instead is more clearly correlated with the hazard factor. Among the different socio-demographic (vulnerability) indicators, the share of young and elderly people is characterized by a negative correlation in all three cities in both the assessments, meaning that these age groups have a tendency (more prominent in London and much less in Sydney) to live in (relatively) less risky areas. In general, London is the city that shows greater correlations (either positive or negative) between all vulnerability indicators and the final risk condition (especially in the heat stress risk assessment), while Sydney is the city that shows lower correlations.

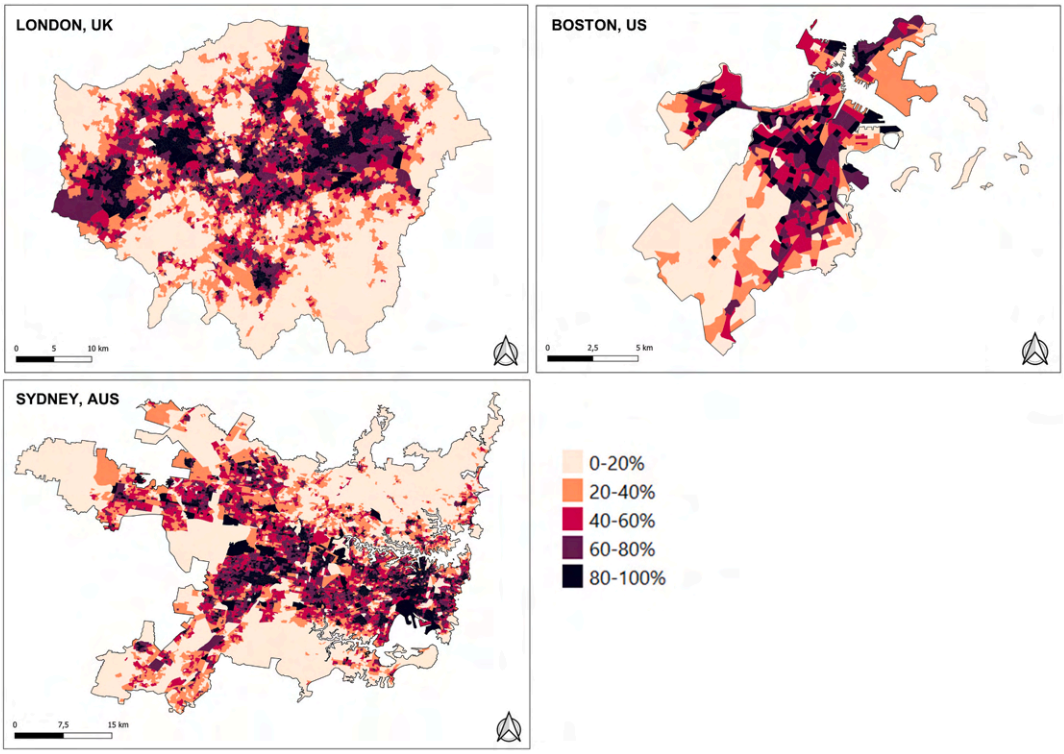


**Fig. 6.** Spatial distribution of the five percentile classes related to the final heat stress vulnerability indicator (i.e., the higher the percentile class, the higher the vulnerability).

To further unveil to what extent the socio-economic disparities may differently contribute to the overall risk in the three cities, an example is provided in Fig. 13 using the income variable (i.e., among the ones showing greater variability among the three cities, with positive values in London and Boston, and negative values in Sydney, see Figs. 11 and 12). The graphic shows the percentage deviation from the overall city average of the median income of the households living in the different heat stress and flood risk conditions according to the five percentile classes of the risk indicator, with the lowest percentile (0–20) indicating the lowest risk condition and the highest percentile (80–100) the highest risk condition. As regards the heat stress risk, the highest and more evident disparities are found in Boston, where households living in lesser risky areas (especially those characterized by the lowest risk condition) have a median income that is nearly 40 % above the city average, while it is the contrary for the riskier areas, with the median income nearly 40 % below the city average in the areas with the highest risk condition. In London too there is a similar pattern (i.e., wealthier households typically living in less risky areas, and the contrary), even if with lower extremes (from above 31 % to below 23 %, approximately), while in Sydney this trend - even if present - is only barely outlined (from above 6 % to below 9 %, approximately). Concerning flood risk, only London shows an unequal distribution among the different risk conditions, with the highest income values (more than 5 % above the city average) found in the less risky areas and a descending trend up to the lowest income values in the riskier areas (22 % below the city average), while this is not true in Boston and Sydney where, instead, most of the risky areas show values above the city average.

Finally, the same analysis was carried out considering the riskiest areas, including those characterized by the highest risk condition for both the hazards (i.e., highest multi-risk). The results reported in Fig. 14 shows that only in London people affected by the worst multi-risk condition are also the ones having the worst economic situation in terms of percentage deviation from the overall city average of the household median income (−28 %), while in Boston and Sydney this happens in areas characterized by the highest risk condition concerning heat stress only.

## 4. Discussion

### *4.1. Potential to support adaptation planning*

Many cities worldwide are increasingly adopting purposeful adaptation strategies and plans (e.g., Ref. [32]) or adaptation-oriented policies and policy instruments into their planning tools (e.g., urban plans [60]) to reduce climate-related risks and/or mitigate impacts.

Adaptation measures may include the use of green-blue infrastructure and nature-based solutions (e.g., green roofs, tree planting, natural water retention areas, etc.) which, through the supply of relevant ecosystem services (e.g., cooling temperatures, surface runoff

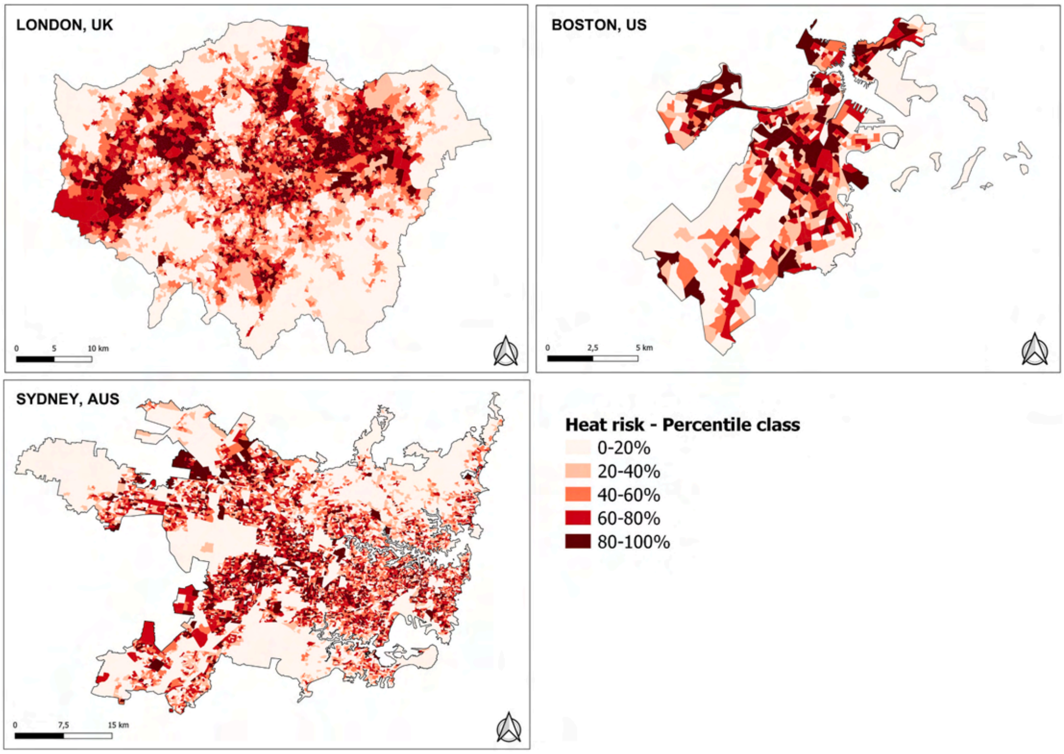


**Fig. 7.** Spatial distribution of the five percentile classes related to the heat stress risk indicator (i.e., the higher the percentile class, the higher the risk).

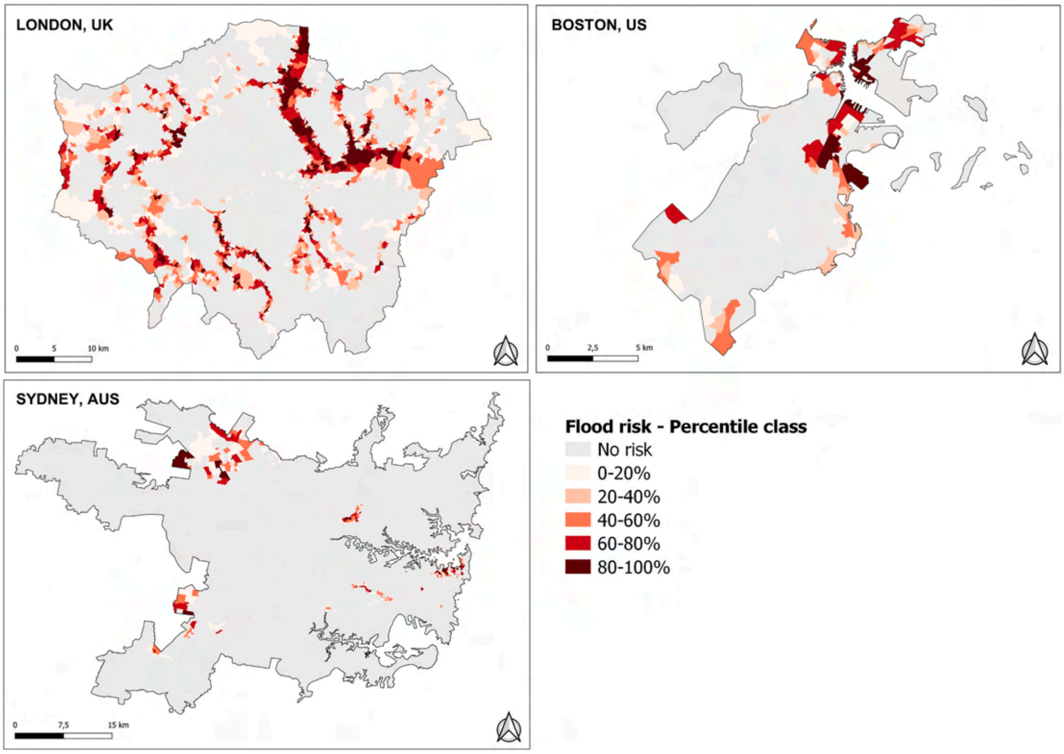


**Fig. 8.** Spatial distribution of the five percentile classes related to the flood risk indicator (i.e., the higher the percentile class, the higher the risk).

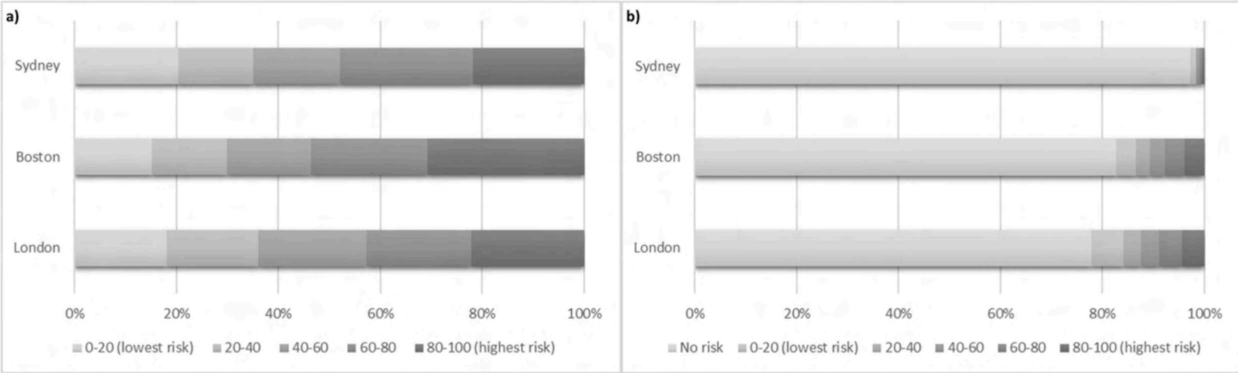


**Fig. 9.** Proportion of resident population per heat stress (a) and flood (b) risk percentile class of the area in which they live.

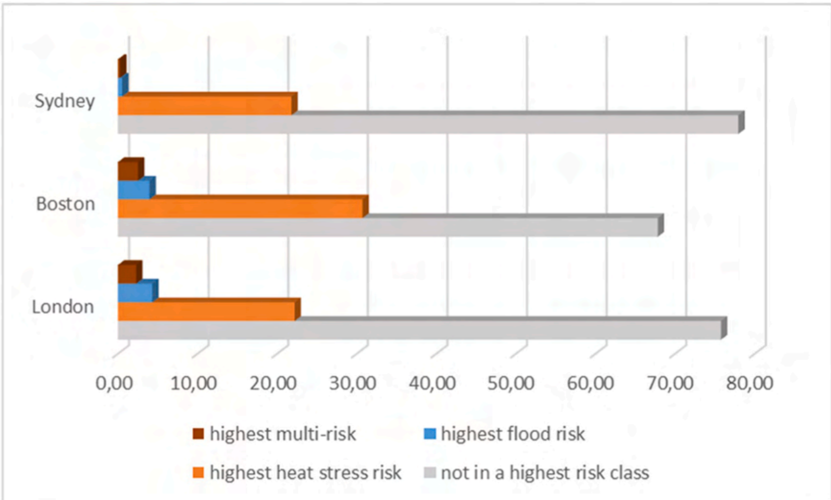


**Fig. 10.** Proportion of resident population living or not in the riskiest areas.

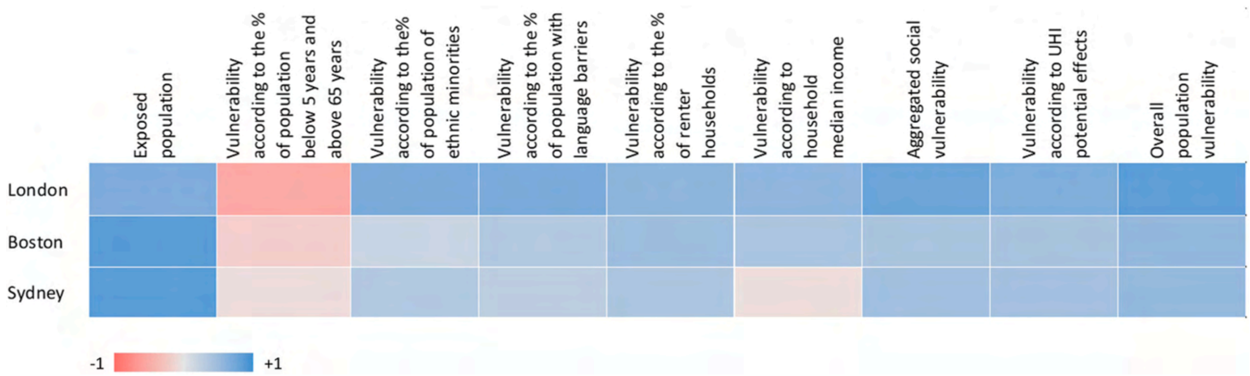


**Fig. 11.** Heatmap of cities (row) and indicators used to calculate the final heat stress risk indicator (columns) based on their correlation with it.

regulation and flood control, etc.), can mitigate climate-related risks and impacts while providing other co-benefits [61]; or the deploy of more engineered (or hybrid) solutions (e.g., Thames barrier, a retractable barrier system built to protect the floodplain of most of Greater London from exceptionally high tides and storm surges [62]). Apart from physical interventions, adaptation solutions may also include soft measures such as the development of early warning systems (e.g., Ref. [63]).

Climate-related risk assessments can support more effective adaptation planning and implementation by providing decision-

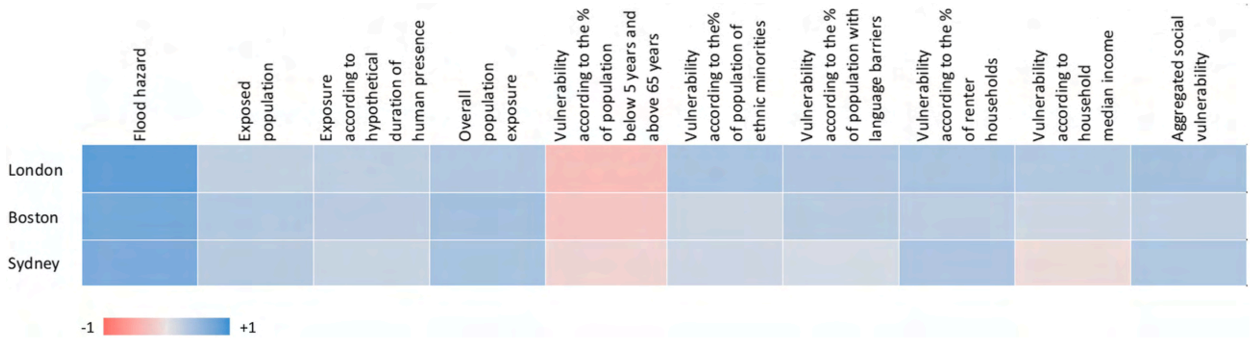


**Fig. 12.** Heatmap of cities (row) and indicators used to calculate the final flood risk indicator (columns) based on their correlation with it.

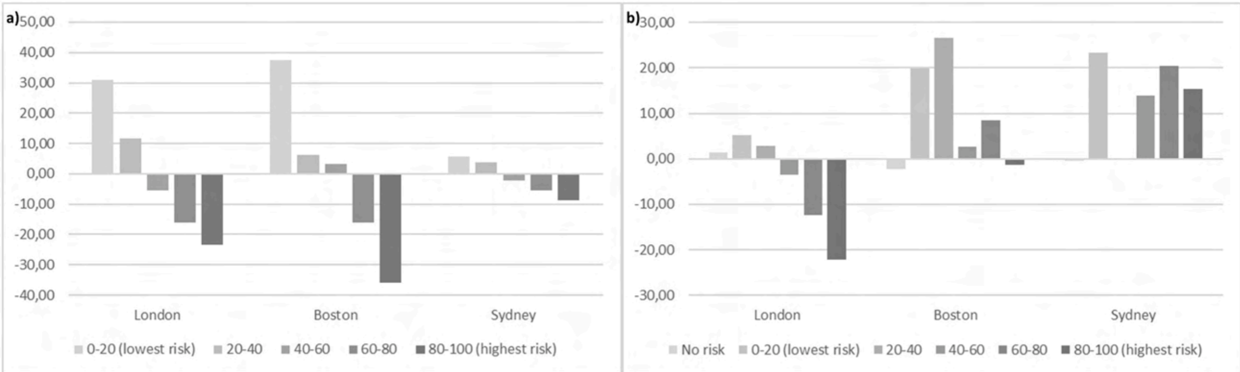


**Fig. 13.** Percentage deviation from the overall city average of the median income of households per heat stress (a) and flood (b) risk percentile class of the area in which they live.

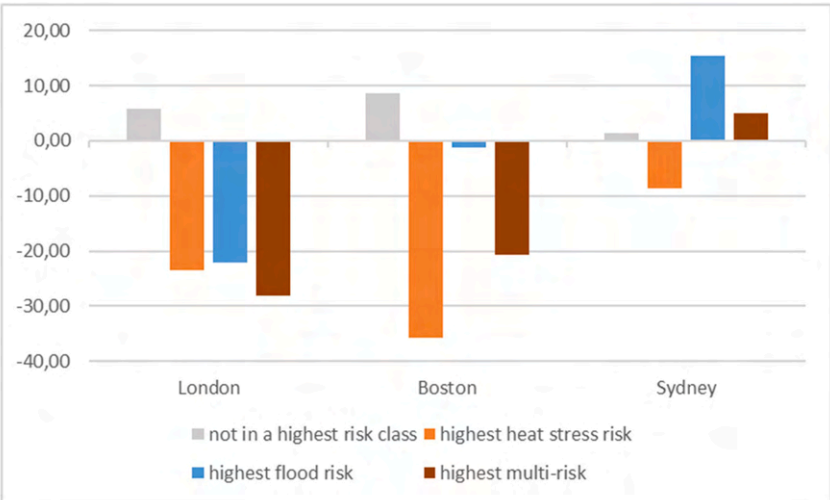


**Fig. 14.** Percentage deviation from the overall city average of the median income of households in and outside the riskiest areas.

makers with spatially explicit information about the areas that need more adaptation (or risk mitigation) measures. They allow the identification of hotspots of risk that may serve as a knowledge base for the (spatial) prioritization and design of adaptation actions within the city policies [64], in line with the scope of similar assessments (e.g., Ref. [65]). This way, efforts and resources can be primarily directed towards these areas to maximize the benefits of adaptation solutions. Taking the proposed assessment as an example (i.e., addressing the risk for the resident population), prioritizing the implementation of a solution in an area characterized by higher risk conditions is likely to provide more benefits (than in less risky areas) in terms of, i.e., a higher number of exposed and/or vulnerable elements that can benefit from it. This means that more people, especially the vulnerable ones who are more likely to be negatively impacted, may experience a risk reduction with a consequent potential decrease of the overall impacts - including health and economic - at the city scale once a hazardous event occurs. Notably, combining the results of more risk assessments (i.e., heat stress and flooding risk, in this case) can lead to identifying multi-risk hotspot areas that need to be adapted with priority. This information can inform not only decisions on the spatial allocation of measures but also the selection of the more suitable ones that can simultaneously tackle multiple (climate-related, but not only) challenges (e.g., Ref. [66]), or their design to maximize multiple risk reduction benefits. For example, in the context of multi-risk, a well-planned green space along an urban river may provide natural retention areas for storing excess water during flood events, vegetated and tree-covered surfaces that cool down temperatures in the surrounding neighborhoods, and a publicly accessible recreation and climate shelter space for the inhabitants – especially the more vulnerable ones that cannot rely on other resources. Nature-based solutions like this one may additionally offer co-benefits such as air purification, carbon sequestration, improved mental health, among others, possibly contributing to many other sustainability goals (e.g., climate mitigation objectives of the Paris Agreement, several specific objectives of SDG11: Sustainable cities and communities, etc.). If such solutions are implemented in a risk hotspot, they would provide their benefits where they are most needed (more deprived areas) and to a high number of vulnerable people, potentially contributing to reducing climate- and environmental-related inequalities.

It has to be noted that the importance of nature-based solutions and urban green infrastructure in the context of climate adaptation (and justice) is already somewhat recognized in all the three case study cities, which are committed to promoting such type of solutions to address climate and other environmental risks, and have adopted specific policies and programmes to this aim (e.g., the Green Infrastructure Policy in the London Plan[10]; the Streets Green Infrastructure Policy and various green infrastructure design guidelines adopted in Boston[11]; or the Greening Strategy,[12] the Urban Forest Strategy,[13] and the Green Grid Strategy[14] of Sydney; see also the city adaptation strategies and policies cited in section 2.1). These strategies and policies could therefore benefit from multi-risk analyses, like the one proposed in this study, that better inform the planning, design, and implementation of multi-objective solutions in contexts of scarce land availability, such as in dense and growing cities.

However, urban plans and policies should not only focus on adapting and reducing the risk of the existing contexts, but also attempt to prevent future risks, considering that urban planning decisions (e.g., location and quality of future urban expansions) are considered among the key factors responsible for the future exposure characterization in a given area [67]. For example, new developments may occur in current or future (due to climate change) flood-prone areas, or at the expense of valuable ecosystems that provide key ecosystem services for local climate risk mitigation, which should indeed deserve protection (or, at least, adequate compensation) to prevent climate-related vulnerabilities/risks from increasing (Hernández & Camerin, 2023).

The proposed risk assessment does not pretend to be the sole instrument for basing adaptation planning decisions. According to Kythreotis and colleagues [34], it should be critically used by decision-makers together with other types of relevant information and knowledge to better reflect on and inform the adaptation choices, avoiding an over-reliance on such technical data, which is characterized by intrinsic limitations (e.g., data availability and reliability/accuracy) and more or less subjective assumptions (e.g., population groups considered more vulnerable, potential weights assigned to the different variables/indicators, etc.). Moreover, it can be adapted to the local context. For example, some socio-demographic variables can be removed if not relevant for a context, or others can be added, and weighting factors can be introduced to additionally weight the different factors considered (e.g., the vulnerability indicators) based on the relative importance they may have for a specific location.

In addition, risk assessments of this type, to some extent, can also be useful to monitor and evaluate the effectiveness of adaptation measures in terms of understanding their beneficial effects on risk reduction. However, with specific regard to the proposed assessment, not all benefits/impacts can be explicitly monitored just by recalculating the indicators using the updated input data obtained after the implementation of a measure. This is partly true only for interventions involving detectable physical transformations and spatial consequences. For example, if a new green space is created or extensive tree planting actions are implemented to counteract UHI, using updated satellite images may be sufficient to detect the 'after implementation changes' according to the heat-island-related vulnerability index; or if a new flood defense system is implemented along a river/the coast, the flood hazard modeled data may be updated taking into account the changes in the flood extent/probability due to the newly implemented measure. For other typologies of intervention, this is not valid. For example, the deployment of early warning systems would not change the risk assessment result, or the implementation of actions to elevate the base of buildings to reduce the risk of being flooded cannot be detected in such a kind of spatial assessment. However, the assessment could be integrated/updated with other variables/indicators (also qualitative) depicting the deployment of soft or other adaptation measures that may reduce the population vulnerability/risk (i.e., usually this type of measures is associated with the so-called adaptive capacity, a subcategory of vulnerability (see, e.g., Ref. [68])).

[10] https://www.london.gov.uk/programmes-strategies/planning/london-plan/the-london-plan-2021-online/chapter-8-green-infrastructure.

[11] https://www.boston.gov/departments/green-infrastructure#:~:text=%E2 %80 %9CGreen%20Infrastructure%E2 %80 %9D%20(GI),absorb%20back%20into%20the%20ground.

[12] https://www.cityofsydney.nsw.gov.au/strategies-action-plans/greening-sydney-strategy.

[13] https://www.cityofsydney.nsw.gov.au/strategies-action-plans/urban-forest-strategy.

[14] https://www.planning.nsw.gov.au/government-architect-nsw/projects-and-collaborations/sydney-green-grid.

### *4.2. Unveiling risk-related inequalities in light of existing evidence and main planning implications*

As shown in Section 3.5, by further analyzing the risk assessment results, it is possible to reveal, at the city scale, what population groups have a more or less pronounced tendency to live within more risky areas. Concerning heat stress risk, people of ethnic minorities and with language barriers are the most overrepresented in London's higher heat stress risk areas, while household renters are the most overrepresented in Boston and Sydney. Contrary, vulnerable age groups quite clearly tend to live in less risky areas in all three cases, a pattern already identified in London and other European cities by Rocha and colleagues (2024). The same study, and another one focused on Greater London [69], also revealed a systematic and significant negative correlation between lower-income populations and the distribution of cooling hotspots in cities that can reduce heat stress risk. This is in line with our findings in London and Boston, while Sydney instead shows almost no correlation between income level and heat stress risk conditions experienced by inhabitants.

A similar pattern can be found in flood risk, with vulnerable age groups tending to live in less risky areas in all three cases, and income level showing nearly no correlation (or even slightly negative) with flood risk in Sydney. However, there is a general tendency of having a lower positive correlation between the presence of vulnerable groups and the level of risk than in the heat stress case. This is especially true concerning the minority ethnic groups and the low-income households, and this tendency is much more evident in Boston than in London. Our findings are (at least partially) corroborated by other studies. For example, one found that in the US the convergence of high flood exposure and high social vulnerability occurs predominantly in the US South and to a much lesser extent in the northern part where Boston is located [70]. Others that in England, instead, the convergence between the likelihood of flooding and deprivation levels of population is high in coastal communities, including the London region [71,72].

Overall, among the three cities analyzed, London seems to be the city in which there is the most pronounced uneven distribution of risk concerning both heat stress and (river and coastal) flood.

Our findings confirm that assessments of this type may be used to unveil potential environmental- and climate-related inequalities due to the uneven distribution of risk conditions among the different population groups. Many vulnerable/disadvantaged groups are more likely to live in more at-risk areas (e.g., low-income populations, particularly evident for heat stress risk in London and Boston, but common also in other cases (e.g. Ref. [36,73])), or, in any case, are the most affected in terms of both health (e.g., mortality is likely higher in low-income populations in case of floods [74] and in low-income, elderly, and minority groups in case of heatwaves [75,76]) and economic damages (e.g., low-income populations typically may not afford flood insurance [77]).

Although the application of risk assessments that consider the social dimension of vulnerability may in principle guide planning decisions that aim to contribute to smoothing out such intra-city inequalities by prioritizing interventions in those disadvantaged areas, this desired outcome is not always automatic, and, in some cases, their implementation may instead lead to exacerbating existing injustices. Especially in cases of green adaptation interventions, the creation of new green space that can theoretically address environmental/climate justice problems can enhance neighborhoods' attractiveness and increase housing costs and property values (e.g., Ref. [78]), a process called (green) gentrification [79]. Ultimately, this process can lead to a displacement of the very residents the interventions were designed to benefit [80], contributing to a pronunciation of existing (or creation of new) injustices [81]. For this reason, great attention should be paid when proposing these types of interventions in less (socially and environmentally) privileged areas, for example by preferring (whenever possible) solutions that involve small-scale interventions and in scattered sites (also called 'just green enough' solutions) rather than only a few big-scale projects that geographically concentrate resources and may kick-start rounds of gentrification [80]. While this especially affects the distributional justice dimension, it is also important to mention the importance of recognitional and procedural justice aspects to avoid reproducing pre-existing inequalities if power imbalances and low involvement of more vulnerable communities in decision-making processes are not adequately addressed, an issue often cited in post-disaster (climate- and non-climate-related) studies (e.g., Ref. [82,83]).

### *4.3. Challenges and limitations of the proposed method*

The risk assessment method proposed does not always use the best knowledge base in each city (e.g., more accurate modeling tools to assess urban temperatures have been developed in several cities, including Boston [84] and London [85], but are not always openly accessible). However, the main objective is to develop and test a method that can be (relatively) easily and freely replicated in many other places, including in those where more accurate data are not available. Consequently, the method is developed to have a fair balance between complexity/accuracy and usability/replicability. However, it is built so that if more accurate data become available or if there is the need to integrate additional risk-related information (e.g., the number of households that have not installed air conditioning systems in their homes, the proximity to shelter places, health status and presence of chronic diseases among residents, which can be used as additional vulnerability factors), these can be pretty easily integrated into the assessment procedure, in line with assessments that used a similar approach (e.g., Ref. [86]).

The main challenge concerns the availability of input data needed to perform the assessment and the frequency with which they are updated. In fact, these types of assessment should be (more or less regularly) updated, given the non-static nature of the phenomena investigated that leads to changes of the risk conditions over time, especially in dynamic or fast-growing urban contexts where demographic transformations, new infrastructure investments, and urban expansion/renewal processes result in frequent changes in vulnerability and exposure variables.

In particular, the availability of socio-demographic data depends on population census information release (i.e., typically every 5–10 years), which is inevitably characterized by a multi-year update frequency and a certain degree of time lag that may not capture potential recent changes in vulnerability [20]. In addition, updated census data does not always include all the necessary information at the finest geographical unit. For example, in London, income data is not available for LSOAs (i.e., the smallest geographical unit for which population data is provided) in the 2021 census survey, leading to the use of the 2011 data. In Boston, the income data from the most updated population survey (i.e., the 2022 American Community Survey) is missing in some city areas, leading to using past year surveys (i.e., 2021 and 2020) to fill the gaps, when possible. Another point is that different national census systems may collect demographic information with different classification approaches. It is the case of the Australian population census survey, which does not explicitly collect data about ethnic/racial groups, such as in the other two cases analyzed (i.e., the US and UK). This poses a series of problems - already recognized by other authors (e.g., Ref. [87]) - linked to the effective classification and measurement of the ethnic and racial identities of census respondents. For this reason, in the Sydney risk assessment, the vulnerability variable concerning ethnic/racial minorities was alternatively derived by analyzing the population ancestry data; each ancestry stated was attributed to a main ethnic/racial group (e.g., White, Black, Asian, Indigenous, etc.), with vulnerable population corresponding to the non-white categories (such as in the cases of London and Boston). This could have led to underestimating or overestimating the likely vulnerable populations in some cases. Another aspect worth mentioning that can lead to over-counting vulnerable residents/households – valid for population vulnerability assessments in general – is the potential for one individual to belong to multiple groups, given that assessment of this type typically quantifies how many people in one specific vulnerable group live in a specific area but not the total number of vulnerable residents [39].

Regarding land use and cover data (used to calculate the exposure indicator in the flood risk assessment), the land use classification and coding systems are very different from one city to another, leading to sometimes hardly defining the category's correspondence between case studies. In one case (i.e., Boston), to have all the necessary land use information for the calculation of the indicator, the integration of different land use and land cover datasets was needed (i.e., the updated city land use and cover map alone does not provide sufficient information for systematically mapping, e.g., open spaces and urban green areas/parks or land dedicated to public buildings and services, leading to using other datasets - the open space map and the regional land use map – to complement the city information).

Flood hazard datasets, too, are developed with different methods in the three cases. They are pretty similar in the UK and US (nationwide datasets), but different in the Australian case. In Sydney, the available regional dataset was used, which is a collection of flood hazard information from different sources, such as local environmental plans. However, from 2021, this dataset is no longer updated, and the single municipalities are in charge of developing and publishing more accurate flood hazard data; therefore, it may not include the latest updates. Interpretations of flood hazard data nomenclature and classes were necessary to homogeneously identify the potential extent of the flood-prone areas that may be inundated in such an event in all the three cases investigated, as well as small assumptions (i.e., in Sydney there are the so-called "flood planning areas" that include land prone to flood where flood-related considerations are required; despite no information is provided about the return period, they were included among the areas that may be in threat during a 100-year-return-period event). It has to be noted that the 100-year flood recurrence period in some cases may be too conservative to inform effective risk reduction due to climate change. However, we used it since available in all three case studies, to ensure consistency of flood extent data across them.

Among the main limitations, it should be noted that all the datasets used (except satellite data that are continuously produced) are developed in a specific past moment and, consequently, provide a photograph of a (more or less recent) past situation (e.g., population and land use data). Consequently, the information they provide may not fully represent the current or near-future situation. For example, socio-demographic data may be different due to population relocations or demographic changes in the years following the census survey [88]; or land use data may not be updated and not include the latest land use changes [89]. However, this is quite a common characteristic of assessments that use these kinds of data (e.g., Ref. [90]), which sometimes leads to finding alternative sources (e.g., alternative population distribution grids [88]). In addition, the replicability of the method heavily depends on the availability of input data, which may not always be available, especially in data-scarce contexts. While, for some information, alternative sources can be found if local data are not available (e.g., globally estimated gridded population count datasets (e.g., WorldPop[15] and Global Human Settlement Layer[16] projects), sometimes including demographic characteristics such as age groups or gender (e.g., WorldPop project)), for others, the availability of detailed local datasets remains crucial or the only option. For example, while open-source global land cover datasets exist (e.g., Copernicus database), only finer local land use data (depicting the distribution of detailed urban uses) can be used for properly assessing the exposure to flood based on the hypothetical temporal duration of human presence. Similarly, specific socio-demographic characteristics such as ethnic groups, income, or house ownership cannot rely on alternative sources other than official surveys, limiting the applicability of the approach when these are not present, or leading to the development of simplified applications that neglect some vulnerability/exposure components. However, it has to be noted that the metrics related to the social vulnerability in this study were selected according to the ones that were considered relevant for and available in all case study cities (among those typically used to mark vulnerable categories), so as to allow a proper comparison of the results. When replicating the assessment in other contexts, such metrics can be adjusted according to the information that is available or more relevant to the local specificities (e.g., Ref. [46]).

Finally, concerning the limitations linked to the resolution of the satellite data used, it has to be noted that while Landsat 8 satellite resolution can capture intra-city variations (of LST and NDVI), it is not suited to detect small-scale vegetation features and surface temperature variations, especially in urban areas where many elements (e.g., streets, buildings, trees, etc.) interact, generating sharp temperature gradients over small distances [91]. This is a general limitation that could affect the results in all three case study cities of

[15] https://www.worldpop.org/.

[16] https://human-settlement.emergency.copernicus.eu/index.php.

the indicator developed to assess the vulnerability to UHI in terms of overlooking finer-scale thermal dynamics between different land uses, built-up spaces, and vegetation.

## 5. Conclusions

Using and combining multi-metric environmental and socio-economic indicators developed with spatially explicit data from different open access sources (i.e., official population census survey, governmental environmental data, satellite data) at the best resolution possible, this study proposes a replicable risk assessment method based on the latest IPCC framework (i.e., risk as a result of hazard, exposure, and vulnerability interplay). The proposed method provides novel insights since many past studies focused on the concept of vulnerability and not risk, or have utilized different approaches than that proposed by the IPCC [92]. To test and show its replicability potential, the method is applied to assess the population risk to be negatively affected by two of the most common climate-related hazards worldwide (i.e., heat stress due to high temperatures and river/coastal flooding) in three cities located in three different continents: London, UK (Europe); Boston, US (North America); and Sydney, Australia (Oceania).

Through an innovative multi-hazard perspective and comparative approach, intra-city risk spatial variability is revealed in the three case studies, together with the factors that, with different magnitudes, contribute to the final risk condition. Possible climate- and environmental-related injustices are also analyzed. Boston has the highest proportion of the population living in the highest risk areas concerning heat stress risk (and the two combined risks), while London regarding flood risk (i.e., flood hazard area extent in London is the largest among the three cities). These two cities also show greater problems of uneven distribution of risk, e.g., with the low-income residents who are also the ones more likely to live in the riskiest areas (for both risks in London, for heat stress risk in Boston). In general, Sydney is the city showing the lowest correlations between the final risk condition and the presence of vulnerable population groups, as well as nearly no sign of unequal distribution of risk. Surprisingly, in all three cases, young children and the elderly (i.e., the most vulnerable to climate-related hazards according to age) tend to live in less risky areas. Despite the resulting spatial variability of risk and its distribution according to vulnerable groups being context-dependent, general lessons learned can be derived. On the one hand, in terms of the suitability of the proposed method (and related assessment techniques and metrics used) to be applied/replicated – through proper local data adjustments and harmonization – in different contexts (with different data sources) having easy access to local environmental and sociodemographic information. In data-scarce contexts, instead, the method could partly rely on alternative sources and/or should be conducted with other metrics. On the other hand, in terms of the variegated situations concerning the uneven distribution of risks across the analyzed cities, which could reflect different prior socio-economic and urban planning dynamics [93]. This can offer an insightful overview for other contexts facing similar situations and thus inform diverse priorities for adaptation and vulnerability reduction, bearing in mind that more detailed analyses on inequality aspects would be most valuable in each case. The application of risk assessments to support planning decisions that prioritize adaptation interventions in more at-risk areas can lead to maximizing benefits in terms of risk reduction (with a consequent expected decrease of the overall impacts and damages experienced by the population at the city scale), possibly contributing to alleviating climate- and environmental-related inequalities. However, decisions towards adaptation need to be taken not only based on tools of this type but also by considering and balancing other aspects not covered by the assessment. This is valid especially because climate risk assessments are characterized by uncertainties and, to some extent, simplification of the complex interrelations between climate/environmental and sociodemographic dynamics.

For these reasons, risk assessments need to be supported by good risk communication to ensure that all the complex interactions, assumptions, and uncertainties associated with climate-related risks are properly communicated to practitioners and end-users together with proper advice for interpretation and application of results [94].

In addition, despite possibly supporting a more just adaptation process, patterns of inequalities may be reiterated due to the triggering of gentrification dynamics, especially in cases of green adaptation interventions implemented in more deprived areas, if no specific measures to avoid them are taken early on in the decision-making process or during early signs of gentrification. Setting up a dedicated monitoring phase during and after the adaptation interventions thus becomes key, both to this aim and to inform possible adjustments in the city adaptation strategies as climate and demographic conditions evolve.

Next steps could include the application of the method with the direct involvement of practitioners and decision-makers to eventually refine it (e.g., discussing and introducing weights in the combination of the different variables/metrics) and to test better the usability and replicability potential of the proposed risk assessment and its results to support effective adaptation planning decisions. Moreover, the method could be applied/integrated for assessing the risk of other exposed population groups (e.g., non-residents, workers at workplaces, etc.), also accounting for population intra-day movements (e.g., population exposure during various times of the day [95]). Finally, a more in-depth analysis concerning potential injustice/inequality aspects linked to climate-related risks could be conducted in each city using the socio-demographic variables already included, and adding new relevant ones, when available, according to their local specificities.

## CRediT authorship contribution statement

**Davide Longato:** Writing – review & editing, Writing – original draft, Visualization, Validation, Resources, Project administration, Methodology, Investigation, Formal analysis, Data curation, Conceptualization. **Denis Maragno:** Writing – review & editing, Writing – original draft, Validation, Supervision, Project administration, Methodology, Funding acquisition, Conceptualization.

## Declaration of competing interest

The authors declare that they have no known competing financial interests or personal relationships that could have appeared to influence the work reported in this paper.

## Acknowledgments

The authors would like to thank Nicola Romanato , researcher at the University Iuav of Venice, for his support in the elaboration of satellite data using the Google Earth Engine platform.

## Appendix A. Supplementary data

Supplementary data to this article can be found online at https://doi.org/10.1016/j.ijdrr.2025.105747.

## Data availability

Data will be made available on request.

## References


[1] IPCC - Intergovernmental Panel on Climate Change, in: H.-O. Pörtner, D.C. Roberts, M. Tignor, E.S. Poloczanska, K. Mintenbeck, A. Alegría, M. Craig, S. Langsdorf, S. Löschke, V. Möller, A. Okem, B. Rama (Eds.), Climate Change 2022: Impacts, Adaptation and Vulnerability. Contribution of Working Group II to the Sixth Assessment Report of the Intergovernmental Panel on Climate Change, Cambridge University Press. Cambridge University Press, 2022, https://doi.org/10.1017/9781009325844.

[2] K. Trenberth, J. Fasullo, T. Shepherd, Attribution of climate extreme events, Nat. Clim. Change 5 (2015) 725–730, https://doi.org/10.1038/nclimate2657.

[3] C. Cheng, Y.C.E. Yang, R. Ryan, Q. Yu, E. Brabec, Assessing climate change-induced flooding mitigation for adaptation in Boston's Charles River watershed, USA, Landsc. Urban Plann. 167 (2017) 25–36, https://doi.org/10.1016/j.landurbplan.2017.05.019.

[4] T.A. Deivanayagam, S. English, J. Hickel, J. Bonifacio, R.R. Guinto, K.X. Hill, M. Huq, R. Issa, H. Mulindwa, H.P. Nagginda, P. de Morais Sato, S. Selvarajah, C. Sharma, D. Devakumar, Envisioning environmental equity: climate change, health, and racial justice, Lancet 402 (10395) (2023) 64–78, https://doi.org/10.1016/S0140-6736(23)00919-4.

[5] K. Dorkenoo, M. Scown, E. Boyd, A critical review of disproportionality in loss and damage from climate change, WIREs Climate Change e770 (2022), https://doi.org/10.1002/wcc.770.

[6] H. Yang, T. Lee, S. Juhola, The old and the climate adaptation: climate justice, risks, and urban adaptation plan, Sustain. Cities Soc. 67 (2021) 102755, https://doi.org/10.1016/j.scs.2021.102755.

[7] EEA, Urban Adaptation to Climate Change in Europe. Challenges and Opportunities for Cities Together with Supportive National and European Policies, EEA Report No 2/2012, European Environment Agency, 2012, https://doi.org/10.2800/41895, 978-92-9213-308-5.

[8] K.L. Ebi, J.J. Hess, Health risks due to climate change: inequity in causes and consequences, Health Aff. 39 (12) (2020) 2056–2062, https://doi.org/10.1377/hlthaff.2020.01125.

[9] C.H. Simpson, O. Brousse, C. Heaviside, Estimated mortality attributable to the urban heat island during the record-breaking 2022 heatwave in London, Environ. Res. Lett. 19 (2024) 094047, https://doi.org/10.1088/1748-9326/ad6c65.

[10] D. Mitchell, C. Heaviside, S. Vardoulakis, C. Huntingford, G. Masato, B.P. Guillod, P. Frumhoff, A. Bowery, D. Wallom, M. Allen, Attributing human mortality during extreme heat waves to anthropogenic climate change, Environ. Res. Lett. 11 (2016) 074006, https://doi.org/10.1088/1748-9326/11/7/074006.

[11] J. Taylor, C. Simpson, O. Brousse, A.K. Viitanen, C. Heaviside, The potential of urban trees to reduce heat-related mortality in London, Environ. Res. Lett. 19 (5) (2024) 054004, https://doi.org/10.1088/1748-9326/ad3a7e.

[12] K. Thomas, R.D. Hardy, H. Lazrus, M. Mendez, B. Orlove, I. Rivera-Collazo, J.T. Roberts, M. Rockman, B.P. Warner, R. Winthrop, Explaining differential vulnerability to climate change: a social science review, Wiley Interdiscip. Rev. Clim. Chang. 10 (2019) e565, https://doi.org/10.1002/wcc.565.

[13] M.A.R. Shah, X. Wang, Assessing social-ecological vulnerability and risk to coastal flooding: a case study for Prince Edward Island, Canada, Int. J. Disaster Risk Reduct. 106 (2024) 104450, https://doi.org/10.1016/j.ijdrr.2024.104450.

[14] S.M. Jibhakate, P.V. Timbadiya, P.L. Patel, Multiparameter flood hazard, socioeconomic vulnerability and flood risk assessment for densely populated coastal city, J. Environ. Manag. 344 (2023) 118405, https://doi.org/10.1016/j.jenvman.2023.118405.

[15] Ö. Ekmekcioğlu, K. Koc, M. Özger, Towards flood risk mapping based on multi-tiered decision making in a densely urbanized metropolitan city of Istanbul, Sustain. Cities Soc. 80 (2022) 103759, https://doi.org/10.1016/j.scs.2022.103759.

[16] E. Yildirim, C. Just, I. Demir, Flood risk assessment and quantification at the community and property level in the state of Iowa, Int. J. Disaster Risk Reduct. 77 (2022) 103106, https://doi.org/10.1016/j.ijdrr.2022.103106.

[17] S. Cheval, A. Dumitrescu, V. Amihăesei, A. Irașoc, M.-G. Paraschiv, D. Ghent, A country scale assessment of the heat hazard-risk in urban areas, Build. Environ. 229 (2023) 109892, https://doi.org/10.1016/j.buildenv.2022.109892.

[18] W. Zhu, C. Yuan, Urban heat health risk assessment in Singapore to support resilient urban design — by integrating urban heat and the distribution of the elderly population, Cities 132 (2023) 104103, https://doi.org/10.1016/j.cities.2022.104103.

[19] R. Paranunzio, E. Dwyer, J.M. Fitton, P.J. Alexander, B. O'Dwyer, Assessing current and future heat risk in Dublin city, Ireland, Urban Clim. 40 (2021) 100983, https://doi.org/10.1016/j.uclim.2021.100983.

[20] F. Li, T. Yigitcanlar, M. Nepal, K. Nguyen, F. Dur, W. Li, Assessing heat vulnerability and multidimensional inequity: lessons from indexing the performance of Australian capital cities, Sustain. Cities Soc. 115 (2024) 105875, https://doi.org/10.1016/j.scs.2024.105875.

[21] G. Cremen, C. Galasso, J. McCloskey, A. Barcena, M. Creed, M.E. Filippi, R. Gentile, L.T. Jenkins, M. Kalaycioglu, E.Y. Mentese, M. Muthusamy, K. Tarbali, R.Š. Trogrlić, A state-of-the-art decision-support environment for risk-sensitive and pro-poor urban planning and design in Tomorrow's cities, Int. J. Disaster Risk Reduct. 85 (2023) 103400, https://doi.org/10.1016/j.ijdrr.2022.103400.

[22] S. Wang, Q.C. Sun, X. Huang, Y. Tao, C. Dong, S. Das, Y. Liu, Health-integrated heat risk assessment in Australian cities, Environ. Impact Assess. Rev. 102 (2023) 107176, https://doi.org/10.1016/j.eiar.2023.107176.

[23] A. Hsu, G. Sheriff, T. Chakraborty, D. Manya, Disproportionate exposure to urban heat island intensity across major US cities, Nat. Commun. 12 (2021) 2721, https://doi.org/10.1038/s41467-021-22799-5.

[24] W.N. Adger, I. Brown, S. Surminski, Advances in risk assessment for climate change adaptation policy, Phil. Trans. R. Soc. A. 376 (2018), https://doi.org/10.1098/rsta.2018.0106.
[25] O.A. Sethamo, M.K. Harder, Evaluating what matters: an evaluation tool for vulnerability risk assessments in local climate change adaptation planning, J. Environ. Plann. Manag. (2021) 1–22, https://doi.org/10.1080/09640568.2020.1866512.
[26] M. Hagenlocher, I. Meza, C. Anderson, A. Min, G. Renaud, Y. Walz, S. Siebert, Z. Sebesvari, Drought vulnerability and risk assessments: state of the art, persistent gaps, and research agenda, Environ. Res. Lett. 14 (8) (2019) 83002–83014, https://doi.org/10.1088/1748-9326/ab225d.
[27] M. Simpson, R. James, J. Hall, et al., Decision analysis for management of natural hazards, Annu. Rev. Environ. Resour. 41 (2016) 489–516, https://doi.org/10.1146/annurev-environ-110615-090011.
[28] C.H.A. Kuran, C. Morsut, B.I. Kruke, M. Krüger, L. Segnestam, K. Orru, T.O. Nævestad, M. Airola, J. Keränen, F. Gabel, S. Hansson, S. Torpan, Vulnerability and vulnerable groups from an intersectionality perspective, Int. J. Disaster Risk Reduct. 50 (2020) 101826, https://doi.org/10.1016/j.ijdrr.2020.101826.
[29] B. Fakhruddin, K. Boylan, A. Wild, R. Robertson, Chapter 12-Assessing vulnerability and risk of climate change, in: J. Sillmann, S. Sippel, S. Russo (Eds.), Climate Extremes and Their Implications for Impact and Risk Assessment, Elsevier, 2020, pp. 217–241, https://doi.org/10.1016/B978-0-12-814895-2.00012-4.
[30] M. Bruno Soares, A.S. Gagnon, R.M. Doherty, Conceptual elements of climate change vulnerability assessments: a review, International Journal of Climate Change Strategies and Management 4 (1) (2012) 6–35, https://doi.org/10.1108/17568691211200191.
[31] R. Córdoba Hernández, F. Camerin, The application of ecosystem assessments in land use planning: a case study for supporting decisions toward ecosystem protection, Futures 161 (2024) 103399, https://doi.org/10.1016/j.futures.2024.103399.
[32] E. Sainz de Murieta, I. Galarraga, M. Olazabal, How well do climate adaptation policies align with risk-based approaches? An assessment framework for cities, Cities 109 (2021) 103018, https://doi.org/10.1016/j.cities.2020.103018.
[33] M. Olazabal, M. Ruiz de Gopegui, E.L. Tompkins, K. Venner, R. Smith, A cross-scale worldwide analysis of coastal adaptation planning, Environ. Res. Lett. 14 (2019) 124056, https://doi.org/10.1088/1748-9326/ab5532.
[34] A.P. Kythreotis, M. Hannaford, C. Howarth, G. Bosworth, Translating climate risk assessments into more effective adaptation decision-making: the importance of social and political aspects of place-based climate risk, Environ. Sci. Pol. 154 (2024) 103705, https://doi.org/10.1016/j.envsci.2024.103705.
[35] A. Jones, J. Kuehnert, P. Fraccaro, et al., AI for climate impacts: applications in flood risk, npj Clim Atmos Sci 6 (2023) 63, https://doi.org/10.1038/s41612-023-00388-1.
[36] Y. Yin, L. He, P.O. Wennberg, C. Frankerberg, Unequal exposure to heatwaves in Los Angeles: Impact of uneven green spaces, Sci. Adv. 9 (2023) eade8501, https://doi.org/10.1126/sciadv.ade8501.
[37] S. Bhattarai, S. Bista, S. Sharma, L.D. White, F. Amini, R. Talchabhadel, Spatiotemporal characterization of heatwave exposure across historically vulnerable communities, Sci. Rep. 14 (2024) 20882, https://doi.org/10.1038/s41598-024-71704-9.
[38] City of Boston, Heat Resilience Solutions for Boston, Final report, 2022. Retrieved from, https://www.boston.gov/sites/default/files/file/2022/04/04212022_Boston%20Heat%20Resilience%20Plan_highres-with%20Appendix%20%281%29.pdf. (Accessed 27 June 2025).
[39] City of Boston, Climate Ready Boston. final report, Retrieved from, https://www.boston.gov/sites/default/files/file/2023/03/2016_climate_ready_boston_report.pdf, 2016. (Accessed 23 October 2024).
[40] City of Sydney, Cooling Sydney strategy, Planning for Sydney 2050 (2019). Retrieved from, https://www.lowcarbonlivingcrc.unsw.edu.au/sites/all/files/publications_file_attachments/sp0012u3_-_cooling_sydney_strategy_final_-_web.pdf. (Accessed 27 June 2025).
[41] O.D. Cardona, M.K. van Aalst, J. Birkmann, M. Fordham, G. McGregor, R. Perez, R.S. Pulwarty, E.L.F. Schipper, B.T. Sinh, Determinants of risk: exposure and vulnerability, in: C.B. Field, V. Barros, T.F. Stocker, D. Qin, D.J. Dokken, K.L. Ebi, M.D. Mastrandrea, K.J. Mach, G.-K. Plattner, S.K. Allen, M. Tignor, P. M. Midgley (Eds.), Managing the Risks of Extreme Events and Disasters to Advance Climate Change Adaptation. A Special Report of Working Groups I and II of the Intergovernmental Panel on Climate Change (IPCC), Cambridge University Press, 2012, pp. 65–108.
[42] A.M. Camarasa-Belmonte, M.J. López-García, J. Soriano-García, Mapping temporally-variable exposure to flooding in small Mediterranean basins using land-use indicators, Appl. Geogr. 31 (2011) 136–145, https://doi.org/10.1016/j.apgeog.2010.03.003.
[43] Autorità di bacino distrettuale delle Alpi Orientali, Aggiornamento e revisione del Piano di Gestione del Rischio di Alluvioni 2021–2027. ALLEGATO I: Elementi tecnici di riferimento nell'impostazione del Piano, 2021. Retrieved from, https://sigma.distrettoalpiorientali.it/portal/index.php/direttiva-alluvioni/pgra-2021-2027/piano_approvato_2021/. (Accessed 17 September 2024).
[44] K. Kim, J. Kang, C. Hwang, Identifying indicators contributing to the social vulnerability Index via a scoping review, Land 14 (2) (2025) 263, https://doi.org/10.3390/land14020263.
[45] J.C. Mah, J.L. Penwarden, H. Pott, O. Theou, M.K. Andrew, Social vulnerability indices: a scoping review, BMC Public Health 23 (1) (2023), https://doi.org/10.1186/s12889-023-16097-6.
[46] D. McCullagh, W. Cámaro-García, D. Dunne, P. Nowbakht, L. Cumiskey, C. Gannon, C. Phillips, Development of a social vulnerability index: enhancing approaches to support climate justice, MethodsX (2025) 103290, https://doi.org/10.1016/j.mex.2025.103290.
[47] Y. Zhao, R. Paul, S. Reid, C.C. Vieira, C. Wolfe, Y. Zhang, R. Chunara, Constructing social vulnerability indexes with increased data and machine learning highlight the importance of wealth across global contexts, Soc. Indic. Res. 175 (2) (2024) 639–657, https://doi.org/10.1007/s11205-024-03386-9.
[48] M.C. Schmidtlein, R.C. Deutsch, W.W. Piegorsch, S.L. Cutter, A sensitivity analysis of the social vulnerability index, Risk Anal. 28 (4) (2008) 1099–1114, https://doi.org/10.1111/j.1539-6924.2008.01072.x.
[49] Z.T. Goodman, C.A. Stamatis, J. Stoler, C.T. Emrich, M.M. Llabre, Methodological challenges to confirmatory latent variable models of social vulnerability, Nat. Hazards 106 (3) (2021) 2731–2749, https://doi.org/10.1007/s11069-021-04563-6.
[50] Bloomberg Associates, London climate risk. A spatial analysis of climate risk across greater London: methodology report. Report prepared for the greater London authority, Retrieved from, https://data.london.gov.uk/download/4ccf1979-51a2-4823-a01d-084f75be5269/ef3176ab-0ef0-41ae-a2b2-d0a5ff3a69af/ClimateRisk_Metadata_2024_092024update.pdf, 2024. (Accessed 27 June 2025).
[51] T.M. Logan, B. Zaitchik, S. Guikema, A. Nisbet, Night and day: the influence and relative importance of urban characteristics on remotely sensed land surface temperature, Remote Sens. Environ. 247 (2020) 111861, https://doi.org/10.1016/j.rse.2020.111861.
[52] M. Santamouris, Recent progress on urban overheating and heat island research. Integrated assessment of the energy, environmental, vulnerability and health impact. Synergies with the global climate change, Energy Build. 207 (2020) 109482, https://doi.org/10.1016/j.enbuild.2019.109482.
[53] D. Longato, D. Maragno, Mapping the vulnerability of urban areas in relation to urban heat island by combining satellite and ecosystem service data: a case study in Udine (Italy), Contesti. Città, Territori, Progetti 2 (2024) 128–149. Retrieved from, https://oajournals.fupress.net/index.php/contesti/article/view/14816. (Accessed 17 September 2024).
[54] V. Lulla, A. Stanforth, N. Prudent, D. Johnson, G. Luber, Modeling vulnerable urban populations in the global context of a changing climate, in: R. Ahn, T. Burke, A. McGahan (Eds.), Innovating for Healthy Urbanization, Springer, Boston, MA, 2015, https://doi.org/10.1007/978-1-4899-7597-3_9.
[55] T. Sun, R. Sun, L. Chen, The trend inconsistency between land surface temperature and near surface air temperature in assessing urban heat island effects, Remote Sens. 12 (8) (2020) 1271, https://doi.org/10.3390/rs12081271.
[56] S.A. Shiflett, L.Y.L. Liang, S.M. Crum, G.L. Feyisa, J. Wang, G.D. Jenerette, Variation in the urban vegetation, surface temperature, air temperature nexus, Sci. Total Environ. 579 (2017) 495–505, https://doi.org/10.1016/j.scitotenv.2016.11.069.
[57] Y. Xiang, B. Zheng, K.M. Bedra, Q. Ouyang, J. Liu, J. Zheng, Spatial and seasonal differences between near surface air temperature and land surface temperature for Urban Heat Island effect assessment, Urban Clim. 52 (2023) 101745, https://doi.org/10.1016/j.uclim.2023.101745.
[58] Z.S. Venter, T. Chakraborty, X. Lee, Crowdsourced air temperatures contrast satellite measures of the urban heat island and its mechanisms, Sci. Adv. 26 (2021) 7, https://doi.org/10.1126/sciadv.abb9569.
[59] M. Pena Acosta, F. Vahdatikhaki, J. Santos, A.G. Dorée, A comparative analysis of surface and canopy layer urban heat island at the micro level using a data-driven approach, Sustain. Cities Soc. 99 (2023) 104944, https://doi.org/10.1016/j.scs.2023.104944.
[60] D. Longato, C. Cortinovis, M. Balzan, D. Geneletti, Identifying suitable policy instruments to promote nature-based solutions in urban plans, Cities 154 (2024) 105348, https://doi.org/10.1016/j.cities.2024.105348.

[61] L. Ruangpan, Z. Vojinovic, J. Plavi, A. Curran, N. Rosic, R. Pudar, D. Savic, D. Brdjanovic, Economic assessment of nature-based solutions to reduce flood risk and enhance co-benefits, J. Environ. Manag. 352 (2024) 119985, https://doi.org/10.1016/j.jenvman.2023.119985.

[62] D. Lumbroso, D. Ramsbottom, Flood risk management in the United Kingdom: putting climate change adaptation into practice in the Thames Estuary, in: Z. Zommers, K. Alverson (Eds.), Resilience: the Science of Adaptation to Climate Change, Elsevier, 2018, pp. 79–87, https://doi.org/10.1016/B978-0-12-811891-7.00006-2.

[63] C. Huggel, M. Rohrer, P. Calanca, N. Salzmann, W. Vergara, N. Quispe, J.L. Ceballos, Early warning systems: the "last mile" of adaptation, Eos Trans. AGU 93 (22) (2012) 209, https://doi.org/10.1029/2012EO220001.

[64] S.K. Allen, J. Ballesteros-Canovas, S.S. Randhawa, A.K. Singha, C. Huggel, M. Stoffel, Translating the concept of climate risk into an assessment framework to inform adaptation planning: insights from a pilot study of flood risk in Himachal Pradesh, Northern India, Environ. Sci. Pol. 87 (2018) 1–10, https://doi.org/10.1016/j.envsci.2018.05.013.

[65] K.F. Tieskens, I.A. Smith, R.B. Jimenez, L.R. Hutyra, M.P. Fabian, Mapping the gaps between cooling benefits of urban greenspace and population heat vulnerability, Sci. Total Environ. 845 (2022) 157283, https://doi.org/10.1016/j.scitotenv.2022.157283.

[66] D. Longato, C. Cortinovis, M. Balzan, D. Geneletti, A method to prioritize and allocate nature-based solutions in urban areas based on ecosystem service demand, Landsc. Urban Plann. 235 (2023), https://doi.org/10.1016/j.landurbplan.2023.104743.

[67] E.Y. Menteşe, G. Cremen, R. Gentile, C. Galasso, M.E. Filippi, J. McCloskey, Future exposure modelling for risk-informed decision making in urban planning, Int. J. Disaster Risk Reduct. 90 (2023) 103651, https://doi.org/10.1016/j.ijdrr.2023.103651.

[68] M. Granceri Bradaschia, D. Longato, D. Maragno, F. Musco, Climate change adaptation mainstreaming through strategic environmental assessments. An in-depth analysis of environmental indicators from spatial plans in Friuli Venezia Giulia Region (Italy), Environ. Impact Assess. Rev. 109 (2024) 107650, https://doi.org/10.1016/j.eiar.2024.107650.

[69] R. Cole, L. Ferguson, C. Heaviside, P. Murage, H.L. Macintyre, J. Taylor, C.H. Simpson, O. Brousse, P. Symonds, M. Davies, S. Hajat, Systemic inequalities in heat risk for greater London, Environ. Int. 190 (2024) 108925, https://doi.org/10.1016/j.envint.2024.108925.

[70] E. Tate, M.A. Rahman, C.T. Emrich, C.C. Sampson, Flood exposure and social vulnerability in the United States, Nat. Hazards 106 (2021) 435–457, https://doi.org/10.1007/s11069-020-04470-2.

[71] Environment Agency, Social Deprivation and the Likelihood of Flooding, Environment Agency, Bristol, 2022. Retrieved from, https://assets.publishing.service.gov.uk/government/uploads/system/uploads/attachment_data/file/1072781/Social_deprivation_and_the_likelihood_of_flooding_-_report_2.1.pdf. (Accessed 21 October 2024).

[72] G. Walker, K. Burningham, Flood risk, vulnerability and environmental justice: evidence and evaluation of inequality in a UK context, Crit. Soc. Policy 31 (2) (2011) 216–240, https://doi.org/10.1177/0261018310396149.

[73] T. Chakraborty, A. Hsu, D. Manya, G. Sheriff, Disproportionately higher exposure to urban heat in lower-income neighborhoods: a multi-city perspective, Environ. Res. Lett. 14 (2019) 105003, https://doi.org/10.1088/1748-9326/ab3b99.

[74] S. Lindersson, E. Raffetti, M. Rusca, L. Brandimarte, J. Mård, G. Di Baldassarre, The wider the gap between rich and poor the higher the flood mortality, Nat. Sustain. 6 (2023) 995–1005, https://doi.org/10.1038/s41893-023-01107-7.

[75] A.A. Williams, J.G. Allen, P.J. Catalano, J.D. Spengler, The role of individual and small-area social and environmental factors on heat vulnerability to mortality within and outside of the home in Boston, MA, Climate 8 (2020) 29, https://doi.org/10.3390/cli8020029.

[76] R. Astone, M. Vaalavuo, Climate change and health: consequences of high temperatures among vulnerable groups in Finland, International Journal of Social Determinants of Health and Health Services 53 (1) (2023) 94–111, https://doi.org/10.1177/00207314221131208.

[77] M. Tesselaar, W.J.W. Botzen, T. Haer, P. Hudson, T. Tiggeloven, J.C.J.H. Aerts, Regional inequalities in flood insurance affordability and uptake under climate change, Sustainability 12 (2020) 8734, https://doi.org/10.3390/su12208734.

[78] F. Camerin, D. Longato, Designing healthier cities to improve life quality: unveiling challenges and outcomes in two Spanish cases, J. Urban Des. (2024) 1–30, https://doi.org/10.1080/13574809.2024.2351925.

[79] A.T. Amorim Maia, F. Calcagni, J. John, T. Connolly, I. Anguelovski, J. Langemeyer, Hidden drivers of social injustice: uncovering unequal cultural ecosystem services behind green gentrification, Environ. Sci. Pol. 112 (2020) 254–263, https://doi.org/10.1016/j.envsci.2020.05.021.

[80] J.R. Wolch, J. Byrne, J.P. Newell, Urban green space, public health, and environmental justice: the challenge of making cities 'just green enough', Landsc. Urban Plann. 125 (2014) 234–244, https://doi.org/10.1016/j.landurbplan.2014.01.017.

[81] A. Haase, K. Koprowska, S. Borgström, Green regeneration for more justice? An analysis of the purpose, implementation, and impacts of greening policies from a justice perspective in Łódź Stare Polesie (Poland) and Leipzig's inner east (Germany), Environ. Sci. Pol. 136 (2022) 726–737, https://doi.org/10.1016/j.envsci.2022.08.001.

[82] R. Córdoba Hernández, F.C. Mateos, J.M. Uriel, F. Camerin, Reconstrucción y resiliencia tras catástrofes naturales: oportunidades perdidas tras la erupción del volcán de Tajogaite en La Palma, Revista De Urbanismo 52 (2025) 1–24, https://doi.org/10.5354/0717-5051.2025.77170.

[83] L.J. Vale, T.J. Campanella (Eds.), The Resilient City: How Modern Cities Recover from Disaster, Oxford University Press, 2005, https://doi.org/10.1093/oso/9780195175844.001.0001.

[84] Klimaat Consulting, Boston Heat Resilience Study. Technical overview of the urban heat island modelling methodology, Retrieved from, https://www.boston.gov/sites/default/files/file/2022/04/Appendix1_CitywideHeatModeling.pdf, 2021. (Accessed 18 September 2024).

[85] ARUP, Urban heat snapshot, Retrieved from, https://www.arup.com/insights/publication-urban-heat-snapshot/, 2024. (Accessed 18 September 2024).

[86] M. Ellena, G. Melis, N. Zengarini, E. Di Gangi, G. Ricciardi, P. Mercogliano, G. Costa, Micro-scale UHI risk assessment on the heat-health nexus within cities by looking at socio-economic factors and built environment characteristics: the Turin case study (Italy), Urban Clim. 49 (2023) 101514, https://doi.org/10.1016/j.uclim.2023.101514.

[87] C. Stevens, F. Fozdar, Ethnicity, race or nation? Census classifications as barriers to the measurement of mixedness in Australia, Australian Population Studies 5 (1) (2021) 49–55, https://doi.org/10.37970/aps.v5i1.81.

[88] N. Wardrop, W. Jochem, T. Bird, H. Chamberlain, D. Clarke, D. Kerr, L. Bengtsson, S. Juran, V. Seaman, A. Tatem, Spatially disaggregated population estimates in the absence of national population and housing census data, Proc. Natl. Acad. Sci. USA 115 (2018) 3529–3537, https://doi.org/10.1073/pnas.1715305115.

[89] R. Prestele, A. Arneth, A. Bondeau, N. de Noblet-Ducoudré, T.A.M. Pugh, S. Sitch, E. Stehfest, P.H. Verburg, Current challenges of implementing anthropogenic land-use and land-cover change in models contributing to climate change assessments, Earth Syst. Dynam. 8 (2017) 369–386, https://doi.org/10.5194/esd-8-369-2017.

[90] C.J. Tomlinson, L. Chapman, J.E. Thornes, C.J. Baker, Including the urban heat island in spatial heat health risk assessment strategies: a case study for Birmingham, UK, Int. J. Health Geogr. 10 (42) (2011), https://doi.org/10.1186/1476-072X-10-42.

[91] R. Andriambololonaharisoamalala, P. Helmholz, I. Ivánová, E. Jones, S. Soon, D. Bulatov, Y. Song, Enhancing the spatial and temporal resolution of satellite-derived land surface temperature in urban environments: a systematic literature review, Urban Clim. 60 (2025) 102345, https://doi.org/10.1016/j.uclim.2025.102345.

[92] A. Shah, K. Malakar, Climate-change-induced risk mapping of the Indian Himalayan districts using the latest IPCC framework, Int. J. Disaster Risk Reduct. 102 (2024) 104283, https://doi.org/10.1016/j.ijdrr.2024.104283.

[93] M. Kalaycıoğlu, S. Kalaycıoğlu, K. Çelik, R. Christie, M.E. Filippi, An analysis of social vulnerability in a multi-hazard urban context for improving disaster risk reduction policies: the case of Sancaktepe, İstanbul, Int. J. Disaster Risk Reduct. 91 (2023) 103679, https://doi.org/10.1016/j.ijdrr.2023.103679.

[94] A. Connelly, J. Carter, J. Handley, S. Hincks, Enhancing the practical utility of risk assessments in climate change adaptation, Sustainability 10 (2018) 1399, https://doi.org/10.3390/su10051399.

[95] Z. Sun, X. Zhang, Z. Li, Y. Liang, X. An, Y. Zhao, S. Miao, L. Han, D. Li, Heat exposure assessment based on high-resolution spatio-temporal data of population dynamics and temperature variations, J. Environ. Manag. 349 (2024) 119576, https://doi.org/10.1016/j.jenvman.2023.119576.